HHS Public Access

Author manuscript

Dev Cell. Author manuscript; available in PMC 2020 December 16.

Published in final edited form as:

Dev Cell. 2019 December 16; 51(6): 787–803.e5. doi:10.1016/j.devcel.2019.10.017.

Adult Drosophila lack hematopoiesis, but rely on a blood cell reservoir at the respiratory epithelia to relay infection signals to surrounding tissues

Pablo Sanchez Bosch[2,#], **Kalpana Makhijani**[2,#,8], **Leire Herboso**[2,#], **Katrina S Gold**[2,#], **Rowan Baginsky**[2,#], **Katie J Woodcock**[4], **Brandy Alexander**[2], **Katelyn Kukar**[2], **Sean Corcoran**[2], **Thea Jacobs**[2], **Debra Ouyang**[2], **Corinna Wong**[2], **Elodie JV Ramond**[6], **Christa Rhiner**[7], **Eduardo Moreno**[7], **Bruno Lemaitre**[6], **Frederic Geissmann**[4,5], **Katja Brückner**[1,2,3,9]

[1]Eli and Edythe Broad Center of Regeneration Medicine and Stem Cell Research, University of California San Francisco, San Francisco, CA [2]Department of Cell and Tissue Biology, University of California San Francisco, San Francisco, CA [3]Cardiovascular Research Institute, University of California San Francisco, San Francisco, CA [4]Kings College London, London, UK [5]Memorial Sloan Kettering Cancer Center, New York, NY [6]EPFL Lausanne, Switzerland [7]Champalimaud Center for the Unknown, Lisbon, Portugal [8]present address University of South Florida Health Byrd Alzheimer's Research Institute, Tampa, FL

Summary

The use of adult *Drosophila melanogaster* as a model for hematopoiesis or organismal immunity has been a matter of debate. Addressing this, we identify an extensive reservoir of blood cells (hemocytes) at the respiratory epithelia (tracheal air sacs) of the thorax and head. Lineage tracing

[9]Corresponding Author and Lead Contact: 35 Medical Center Way, San Francisco, CA 94143-0669, katja.brueckner@ucsf.edu.

Author Contributions

This study was made possible by the combined talent of all authors over the course of more than ten years. PSB expertly planned, performed and statistically analyzed the majority of qPCR experiments, added the aspect of Upd3/Jak/Stat signaling, contributed some survival data, and majorly revised qPCR figures. KM expertly planned and generated complex *Drosophila* genotypes and planned, performed and analyzed lineage tracing, MARCM, EdU, hemocyte quantification and marker experiments, and provided key information on the *Drosophila* respiratory epithelia. LH creatively developed new ways to visualize *Drosophila* adult respiratory epithelia, and planned, performed and analyzed adult fly dissections, confocal microscopy, microbead and bioparticle localization, phagocytosis assays, qPCR and survival experiments. KG planned, performed and analyzed experiments related to tissue colocalizations, microbead localization, confocal imaging, EdU incorporation, reporter and marker analyses, qPCR experiments, and contributed to the writing of the manuscript. RB planned, performed and analyzed whole and split-fly hemocyte counts and –qPCRs, and other qPCR and initial survival experiments. BA developed and performed fly cryosectioning, and performed EdU, lineage tracing, dye and marker experiments. KK performed and analyzed survival experiments. SC performed and analyzed experiments related to fly infections, bioparticle injections, and pHrodo counts. TJ performed qPCR experiments. DO performed survival experiments. CW performed fly sectioning and staining. KW and FG generated and contributed valuable *Fucci* transgenic lines, and expert hemocyte quantification, Fucci analyses and confocal images. CR and EM kindly contributed the PermaTwin system prior to its publication. EJVR and BL trained KB in *Drosophila* infection techniques and assays, and generously provided wide-reaching expert advice and materials. KB conceived the study, guided lab members, discovered the anatomical link of hemocytes and respiratory epithelia, planned experiments, analyzed data, generated figures, and wrote the manuscript. All authors provided input on the manuscript.

[#]Equal contribution, in reverse alphabetical order

Declaration of Interests

The authors declare no competing interests.

and functional analyses demonstrate that the majority of adult hemocytes are phagocytic macrophages (plasmatocytes) from the embryonic lineage that parallels vertebrate tissue macrophages. Surprisingly, we find no sign of adult hemocyte expansion. Instead, hemocytes play a role in relaying an innate immune response to the blood cell reservoir: through Imd signaling and the Jak/Stat pathway ligand Upd3, hemocytes act as sentinels of bacterial infection, inducing expression of the antimicrobial peptide *Drosocin* in respiratory epithelia and colocalizing fat body domains. *Drosocin* expression in turn promotes animal survival after infection. Our work identifies a multi-signal relay of organismal humoral immunity, establishing adult *Drosophila* as model for inter-organ immunity.

Graphical Abstract

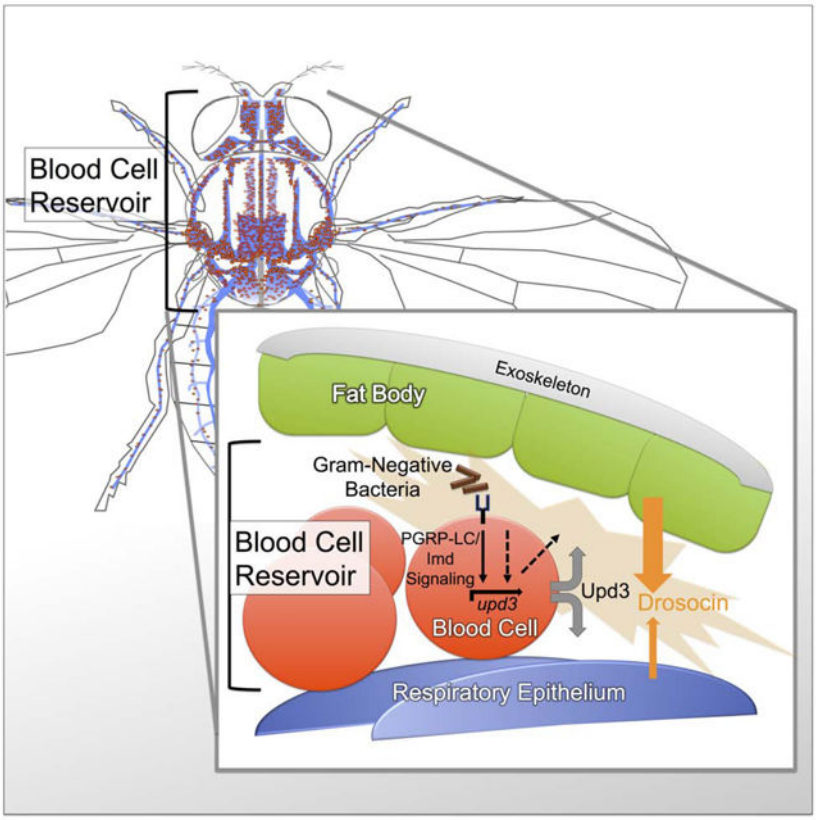

eTOC Blurb

Sanchez Bosch et al. study hemocytes (blood cells) in the adult *Drosophila* system. They do not find hematopoiesis in the adults, but they do identify hemocyte reservoirs at respiratory epithelia and the fat body and show that cells at these reservoirs mediate a local humoral immune response to bacterial infection.

Keywords

Drosophila melanogaster; hemocyte; macrophage; respiratory epithelia; tracheal air sacs; fat body; hematopoiesis; blood cell reservoir; innate immunity; NFκB; *imd*; *upd3*; Jak/Stat; *hop*; *Stat92E*; local humoral immune response; antimicrobial peptide; *Drosocin*

Introduction

Drosophila melanogaster has greatly promoted our understanding of innate immunity and blood cell development, but the capacity of the adult animal as a model remains a matter of debate. Most studies reported lack of new blood cell production (Lanot et al., 2001; Mackenzie et al., 2011; Woodcock et al., 2015) and increasing immunosenescence (Felix et al., 2012; Mackenzie et al., 2011), while one publication claimed continued hematopoietic activity in adult *Drosophila* (Ghosh et al., 2015).

Drosophila blood cells, or hemocytes, emerge from two lineages that persist into the adult, showing parallels with the two myeloid systems in vertebrates (Gold and Brückner, 2014, 2015; Holz et al., 2003). First, hemocytes originating in the embryo parallel vertebrate tissue macrophages, as they quickly differentiate into plasmatocytes (macrophage-like cells), and subsequently proliferate extensively, mainly in the hematopoietic pockets (HPs) of the larva (Gold and Brückner, 2014, 2015; Makhijani et al., 2011; Makhijani and Brückner, 2012). At least some of these plasmatocytes can further differentiate into other blood cell types such as crystal cells and, under immune challenge, lamellocytes (Bretscher et al., 2015; Gold and Brückner, 2015; Leitao and Sucena, 2015; Makhijani et al., 2011; Markus et al., 2009). Second, hemocytes originating in the lymph gland (LG) also give rise to plasmatocytes, crystal cells and lamellocytes, yet in the lymph gland they are predominantly generated from blood cell progenitors (prohemocytes) (Banerjee et al., 2019; Gold and Brückner, 2015; Jung et al., 2005; Letourneau et al., 2016). At the beginning of metamorphosis, hemocytes from both the hematopoietic pockets and the lymph gland enter the open circulatory system and intermix (Gold and Brückner, 2015; Grigorian et al., 2011; Lanot et al., 2001; Makhijani et al., 2011). The subsequent fate and capacity of the adult blood cells has been a matter of debate. Accordingly, we dedicated the first part of our study to comprehensively investigate the hematopoietic capacity of the blood cell system in adult *Drosophila*. For the second part of the study, we focused on the role of adult blood cells in the humoral immune response, identifying a system of organismal innate immunity that centers on the respiratory epithelia in *Drosophila*.

Historically, *Drosophila* has been instrumental in the discovery of innate immunity and Toll like receptor (TLR) signaling (Lemaitre and Hoffmann, 2007). Toll- and the related Immune Deficiency (Imd) signaling are evolutionary conserved NFκB family pathways, studied in detail regarding their upstream activation by pathogens and other inputs, and downstream signal transduction components and mechanisms (Lemaitre and Hoffmann, 2007). Targets include antimicrobial peptides (AMPs), which have been investigated for their transcriptional gene regulation and functional properties (Lemaitre and Hoffmann, 2007; Zasloff, 2002). TLR signaling has been well established also in vertebrate systems for its roles in infection and inflammation (Beutler, 2009; Kopp and Medzhitov, 1999; Takeda and Akira, 2005). However, it has been far less understood how multiple tissues or organs communicate with each other to elicit local innate immune responses.

This study clarifies basic principles of the blood cell system in adult *Drosophila* and its role in multi-tissue organismal immunity. We identify an extensive blood cell reservoir at the

respiratory epithelia and fat body, investigate its dynamics, and probe for various signs of hematopoiesis. We demonstrate a key role of adult blood cells as sentinels of bacterial infection that trigger a humoral response in their reservoir, i.e. the respiratory epithelia and colocalizing domains of the fat body. This response culminates in the expression of the AMP gene *Drosocin*, which we show is significant for animal survival after bacterial infection. Our work identifies Imd signaling and Upd3 expression in hemocytes as required steps in this relay of organismal immunity, laying the foundation for the use of adult *Drosophila* to dissect additional mechanisms of multi-tissue innate immunity in the future.

Results

The respiratory epithelia provide the largest reservoir of blood cells in adult Drosophila

Investigating the blood cell system in adult *Drosophila*, we examined the anatomical sites of hemocytes. We visualized blood cells by fluorescent labeling with macrophage (plasmatocyte)-specific *Hemolectin Hml*Δ-*GAL4* (Sinenko and Mathey-Prevot, 2004) driving *UAS-GFP*, or direct reporters *Hml*Δ-*DsRed* or *Hml*Δ*DsRednls* (Makhijani et al., 2011). To gain an unbiased overview of hemocyte locations throughout the animal, we took a cryosectioning approach. In addition, we imaged hemocytes through the cuticle of intact flies. Hemocytes are largely resident (sessile) and enriched in specific areas. Surprisingly, we found that the largest pool of hemocytes colonizes the respiratory epithelia, in particular the extensive air sacs of the thorax and head (Fig. 1A–E). This was identified in cryosections by comparison with anatomical features of the respiratory epithelia (Manning and Krasnow, 1993; Whitten, 1957), and the unique blue autofluorescence of the respiratory epithelia when exposed to UV light (Kim et al., 2012). Localization of hemocytes with the respiratory epithelia was further confirmed by colabeling with the tracheal driver *btl-GAL4* expressing *UAS-GFP* (Guha and Kornberg, 2005) (Fig. 1D, Suppl.Fig. 1C). In intact flies, hemocyte localization at the respiratory epithelia is visible around the eyes and posterior head, and in the thorax laterally, and dorsally near the wing hinges and scutellum (Suppl. Fig. 1A,C,D).

Consistent with previous reports (Dionne et al., 2003; Elrod-Erickson et al., 2000; Ghosh et al., 2015), we also saw a smaller fraction of hemocytes surrounding the heart (Suppl.Fig. 1A,B,D), accumulating in clusters at the ostia (Suppl. Fig.1B), i.e. the intake valves toward the open circulatory system. Quantification of hemocytes released from flies split into two parts, at the boundary of the thorax and abdomen, confirmed that the majority of hemocytes in adult *Drosophila* is located in the head and thorax (see Fig. 3F). Overall we conclude that, in adult *Drosophila*, the respiratory epithelia of the head and thorax provide the major reservoir of blood cells, which is distinct from smaller clusters of hemocytes at the heart.

Hemocytes relocate during maturation of adult Drosophila

Next we investigated the developmental timing of hemocyte localization to the respiratory system and heart. Newly eclosed *Drosophila* expressing a fluorescent plasmatocyte reporter show a diffuse glow in live imaging, which over the following 5–7 days develops into a more defined hemocyte pattern (Fig. 2B–C). In these mature adults, hemocytes then remain stationary over time (Suppl. Fig2A–C and (Woodcock et al., 2015)). While the visual change of hemocytes in young adults may suggest an increase in total hemocyte numbers, we

actually found a different underlying cause. Specifically, we discovered a major redistribution of hemocytes within the first days of adult life. Dissection and lipid dye staining of newly eclosed adults illustrates that hemocytes are attached to dissociated larval fat body cells (Fig. 2D) (Nelliot et al., 2006), forming a large mass throughout the abdomen and other parts of the fly (Fig. 2E). Around 5–7 days into adult life, cytolysis of the larval fat body cells is completed, allowing hemocytes to relocate to resident sites at the respiratory system and heart (Fig. 2F). Consequently, local hemocytes, e.g. in the heart area, increase during the first days of adult life (Fig. 2E–F dashed box), and fluorescently labeled hemocytes that can be visually recognized through the external cuticle transiently increase (Fig. 2G). However, when assessing hemocytes in cryosections (Fig. 2E–F), or quantifying total hemocytes from dissected adult flies, we discovered a continuous decline in hemocytes over various time points, even during the first week of adult life (Fig. 2H and (Woodcock et al., 2015)). Accordingly, we find no evidence for a significant increase in total hemocytes during adult maturation. Instead, we observe redistribution of existing hemocytes during the first week of adult life: Once larval fat body cells have cytolysed, hemocytes move toward the periphery to their final destinations at the respiratory epithelia and the heart.

Hemocytes do not expand after septic injury

Next we investigated whether bacterial infection could have an effect on hemocytes of the respiratory system and the heart (Fig. 3B, C). Injection of adult flies with gram-negative *Escherichia coli (E.coli)*, *Erwinia carotovora carotovora 15* (*Ecc15*), or gram-positive *Micrococcus luteus (M. luteus)* resulted in increased hemocytes visible through the cuticle 6 days post infection (Fig. 3C, D). However, we discovered that absolute hemocyte numbers, quantified by total blood cell release, did not increase upon infection (Fig. 3E). Asking whether hemocytes may redistribute upon infection, we assessed blood cell counts from flies split into 2 parts, i.e. head plus thorax, versus abdomen (Fig. 3F). Similar as in maturation, bacterial immune challenge did not affect absolute hemocyte numbers in the two sections; there was no effect of the site of injection in the thorax or abdomen (Fig. 3F). Tracking down what could be the basis for the seemingly increased hemocyte appearance after infection, we found that bacterial infection leads to transcriptional upregulation of macrophage-specific *Hml* and other commonly used marker genes such as *croquemort (crq)* (Fig. 3G), as has been described previously (De Gregorio et al., 2001; Franc et al., 1999). Increased *Hml*Δ reporter expression after bacterial infection likely accounts for elevated GFP levels, increasing the number of hemocytes that can be visually recognized through the cuticle, while absolute hemocyte counts are not raised.

To further address the role of the respiratory hemocyte reservoirs in infection, we examined the dynamics of particle accumulation, injecting fluorescently labeled microbeads or *E. coli* bioparticles. Independent of the site of injection in the thorax or abdomen, particles quickly accumulate along the respiratory epithelia of the thorax and head (Fig. 3H–Q), and at the ostia of the heart (Fig. 3H,I), matching typical sites of hemocyte residence. Comparable localization of particles was observed under hemocyte ablation conditions (Suppl. Fig. 3B), suggesting that this pattern is independent of hemocyte phagocytosis. However, hemocytes at the respiratory epithelia are active phagocytes, as they ingested bioparticles marked with regular label (Fig. 3S) or pHrodo, a pH dependent dye highly fluorescent in acidic

compartments such as lysosomes (Suppl. Fig. 3C). Fractions of pHrodo positive hemocytes released from head, thorax or abdomen of split flies were similar (Fig. 3R, T-V), suggesting comparable phagocytic activity and similar ratios of hemocyte- and particle accumulation in all body parts.

In summary, we find major accumulation of foreign particles in the hemocyte reservoirs lining the respiratory epithelia of *Drosophila*. This localization is independent of the presence of phagocytes, suggesting passive transport through the hemolymph and physical retention in these areas. Bacterial infection does not substantially change the overall localization of hemocytes, and does not cause significant increase in the total number of hemocytes per animal. Instead, we find a substantial increase in the expression of macrophage markers, likely accounting for the increased appearance of hemocytes that are visible though the cuticle.

The majority of adult hemocytes derive from the embryonic lineage

Next we sought to determine the ontogenesis of the adult blood cell system. Blood cells in adult *Drosophila* are known to derive from two lineages (Holz et al., 2003), the embryonic lineage that parallels tissue macrophages, and the lymph gland lineages that parallels progenitor-based blood cell production (Fig. 4A) (Banerjee et al., 2019; Gold and Brückner, 2014, 2015). To address their relative contributions to the adult animal, we used a flipout-*lacZ* lineage tracing approach (Makhijani et al., 2011; Weigmann and Cohen, 1999): Spatially and temporally controlled Flp recombinase induces reconstitution and permanent expression of a lacZ reporter transgene, which can be followed and compared relative to other cell markers. First, we marked early embryonic hemocytes (under control of *srpHemo-Gal4*) and examined animals at the pupal and adult stage (Fig. 4B–E). This resulted in many *lacZ* positive hemocytes in the pupa (Fig. 4D,D') and in the adult, including hemocytes attached to larval fat body cells in newly eclosed flies (Fig. 4E). We obtained similar results when labeling differentiated embryonic-lineage plasmatocytes in the young larva using *Hml*Δ-*GAL4* (Fig. 4F–I). The method further allowed to quantify contribution of embryonic-lineage hemocytes to the adult blood cell pool. Comparing the fraction of *lacZ* positive cells among plasmatocytes in the adult relative to those in the 3rd instar larva, we estimate that more than 60% of adult macrophages originate from the embryonic lineage (Fig. 4I) that proliferates in the larva and resembles tissue macrophages in vertebrates (Gold and Brückner, 2014, 2015; Makhijani et al., 2011; Makhijani and Brückner, 2012). Based on our findings we expect that less than 40% of adult hemocytes derive from the lymph gland lineage, although we can only infer this contribution as the relatively weak expression of early lymph gland GAL4 drivers left our lineage tracing attempts of the lymph gland unsuccessful.

Adult Drosophila show no signs of new hemocyte production

Given that adult hemocytes originate from embryonic-lineage hemocytes, which retain the ability to proliferate as macrophages in the larva (Makhijani et al., 2011), and the lymph gland lineage, which includes undifferentiated progenitors from the posterior lobes (Grigorian et al., 2011; Jung et al., 2005), we investigated the proliferative capacity and differentiation of adult hemocytes. First we used in vivo EdU (5-ethynyl-2'-deoxyuridine)

incorporation into newly synthesized DNA to detect proliferation of macrophages and their putative progenitors. Labeling EdU-incorporating cells over two weeks and examining the entire pool of adult hemocytes ex vivo, we surprisingly did not find any EdU positive hemocytes (Fig. 5A). Fragments of other tissues that are side products of the hemocyte release method harbored EdU positive cells, serving as positive control (Fig. 5A). To explore the possibility of hemocytes or their progenitors proliferating upon immune challenge, we challenged adults by natural infection (feeding) with the gram-negative bacterium *Serratia marcescens (S. marcescens)*, or septic injury using gram-negative *E. coli*, *Ecc15*, or gram-positive *M. luteus*. Even upon infection, we did not detect any EdU positive hemocytes (Fig. 5A). Some hemocytes carried EdU positive cellular inclusions other than their own nucleus, indicating phagocytosis of other EdU-incorporating polyploid or proliferative cells (Suppl. Fig. 4G–I). This suggests that neither differentiated macrophages, nor potential unlabeled progenitors that may give rise to macrophages, proliferate under the tested conditions.

We sought numerous other methods to detect proliferation of plasmatocytes or their progenitors. Using a hemocyte-specific two-color Fucci cell cycle indicator line, we found no Fucci S/G2/M green-positive hemocytes in adult flies (Fig. 5C-F'), while proliferating larval hemocytes served as positive control (Fig. 5B-B'). Likewise, hemocyte MARCM (Mosaic analysis with a repressible cell marker) (Lee and Luo, 1999; Makhijani et al., 2011), which labels all dividing cells that eventually would give rise to hemocytes (Suppl. Fig. 4A), resulted only in minimal numbers of MARCM positive hemocytes; rare events could simply be due to the high background labeling seen under all induction conditions (Suppl. Fig. 4B, C) and in other systems (von Trotha et al., 2009). Lastly, PermaTwin labeling, a MARCM variant designed to detect all dividing cell progeny (Fernandez-Hernandez et al., 2013), did not produce any labeled hemocytes over induction periods of up to 3 weeks, as we determined by external imaging of intact flies and hemocyte releases. As expected, the method generated many positive cells in control tissues such as the gut (Suppl.Fig. 4D, E).

We also examined adult flies for putative hemocyte progenitors. We focused on Srp, a GATA factor required for prohemocyte specification in the embryo (Rehorn et al., 1996), which was recently proposed as progenitor marker in the adult fly (Ghosh et al., 2015). We examined Srp-positive hemocytes using a Srp antibody or *srp-GAL4* driver, both of which labeled very similar, overlapping populations of hemocytes in young and more mature adults (Suppl.Fig. 4F). Surprisingly, we found that most Srp-positive hemocytes in the adult show hallmarks of phagocytosis, including internal phagocytic vesicles and the ability to phagocytose experimentally injected fluorescent microbeads (Fig. 5I–M). In maturing adults between day 3 and 11 after eclosion, an increasing number of Srp-positive hemocytes also gained expression of the plasmatocyte marker *HmlΔDsRednls* (Fig. 5G, H). However, even single positive Srp-only hemocytes are largely capable of ingesting injected beads (Fig. 5J, L), similar to *Hml* positive or double positive cells (Fig. 5K,M).

We conclude that, in the adult fly, Srp is not a marker for hemocyte progenitors. Overall, we find no indication that the adult blood cell system has significant hematopoietic capacity. Instead, we observe mainly active macrophages and a continuous decline of blood cell numbers in adult animals. Accordingly, we propose that the adult blood cell pool results

from hemocyte expansion in the larva, and over time diminishes without any significant new blood cell production (Fig. 5N).

Hemocytes, through cell-autonomous Imd signaling, are required for an infection-induced Drosocin response

Focusing on the purpose and anatomical arrangement of hemocytes at the respiratory epithelia, we investigated consequences for humoral immunity. Comparing hemocyte-ablated and control animals, we examined transcriptional induction of antimicrobial peptide (AMP) genes following bacterial infection. Hemocyte ablation was achieved by expression of the proapoptotic genes *reaper* (*rpr*) and *head involution defect* (*hid*) (Arefin et al., 2015; Bergmann et al., 1998; Charroux and Royet, 2009; Defaye et al., 2009; White et al., 1996) and confirmed through live imaging of larvae and adults and quantification of released hemocytes (Suppl.Fig. 5A,B). *E. coli* was selected for these infections, owing to its use for gram-negative infection in similar *Drosophila* studies (Ghosh et al., 2015; Lemaitre and Hoffmann, 2007). Following septic injury in the absence of hemocytes, we found that expression of *Drosocin* was consistently reduced under hemocyte-ablated conditions, suggesting dependence on hemocytes (Fig. 6A). Using a *Drosocin-GFP* transgenic reporter (Tzou et al., 2000), we found a unique expression pattern in the thorax and head of infected flies that strikingly matched locations of the hemocyte reservoir at the respiratory epithelia (Fig. 6B–D) and differed from a general fat body expression pattern (Fig. 6E). This *Drosocin-GFP* pattern was independent of the site of bacterial injection in the thorax or abdomen (Suppl.Fig. 6A,B). We confirmed the localized *Drosocin* expression by qPCR analysis on infected flies split into two parts, i.e. head and thorax, versus abdomen (Fig. 6F).

Focusing on *Drosocin* expression as a paradigm, we examined requirement for the NFκB-related Imd signaling pathway for detection and response to gram-negative bacteria in hemocytes. Indeed, constitutive *imd* knockdown in hemocytes dramatically reduced *Drosocin* expression following gram-negative infection at various time points post infection (Suppl.Fig. 5C,D). Similar results were obtained when we silenced *imd* only transiently before infection (Fig. 6G), ruling out that a general shift in the immune status (Arefin et al., 2015) would cause the observed phenotype. Likewise, hemocyte-specific knockdown of the upstream peptidoglycan receptor *PGRP-LC* substantially reduced *Drosocin* induction (Fig. 6H), suggesting that recognition of bacterial cell wall components such as DAP-type peptidoglycan is required to trigger the response (Kaneko et al., 2006). Overexpression of *imd*, which leads to pathway activation (Georgel et al., 2001), mildly enhanced *Drosocin* expression after sterile and septic injury (Fig. 6I, Suppl.Fig. 5E) consistent with the Imd pathway in hemocytes being required, albeit not sufficient, for the response.

We conclude that, in response to gram-negative infection, hemocytes are essential players in the induction of humoral immunity. Signaling through the PGRP-LC/Imd pathway in hemocytes is required, albeit not sufficient, for the *Drosocin* response.

Hemocytes act as sentinels of infection that induce Drosocin expression in the respiratory epithelia and fat body

Next we asked in which tissues *Drosocin* would be expressed. Dissection revealed that *Drosocin-GFP* is expressed in the respiratory epithelia and in adjacent domains of the fat body, which overlays the respiratory epithelia and fills the space toward the exoskeleton (Fig. 7A-A", see also Fig. 7E-F'''). This restriction to specific fat body domains was particularly obvious when comparing *Drosocin-GFP* to the overall expression of a fat body driver (Fig. 6E). No striking expression of *Drosocin-GFP* was detected in hemocytes in vivo or ex vivo (Fig. 6C, 7A and data not shown).

To further confirm contribution of these tissues to the overall *Drosocin* response, we performed tissue specific RNAi knockdowns of *Drosocin* and analyzed total *Drosocin* expression by qPCR of whole flies. Silencing of *Drosocin* in the respiratory system shows partial contribution to the total *Drosocin* expression (Fig. 7C). Silencing of *Drosocin* in fat body demonstrated that the major contribution comes from this tissue (Fig. 7D), consistent with the observed high levels of *Drosocin-GFP* expression in fat body, and its established role as major site of AMP expression. In contrast, *Drosocin* silencing in hemocytes caused little to no reduction in overall *Drosocin* levels, again illustrating that hemocytes themselves are not a significant source of total *Drosocin* expression in the fly (Fig. 7A). Overall *Drosocin* knockdown efficiency was close to 100% using a ubiquitous driver (Suppl.Fig. 6D).

Considering that hemocytes are required for *Drosocin* induction, yet *Drosocin* is predominantly expressed in domains of the fat body and the respiratory epithelia, we hypothesized that hemocytes might act as sentinels of infection that signal through some molecular mechanism to the *Drosocin*-expressing tissues. Cryosections of whole adult animals and head dissections show that hemocytes tightly colocalize with, and are layered in between, the respiratory epithelia and fat body, suggesting an interface that facilitates signaling communications among the tissues (Fig. 7E-F''', Suppl.Fig. 6C,C'). Hypothesizing communication via a secreted factor, we tested potential candidate genes of secreted signaling molecules by RNAi and overexpression. One gene that stood out was *unpaired 3* (*upd3* (Agaisse et al., 2003)), a ligand of the Jak/Stat pathway. Hemocyte specific knockdown of *upd3* strongly reduced *Drosocin* expression after gram-negative infection (Fig. 7G), suggesting that Upd3 is a required hemocyte produced signal in the communication to the respiratory epithelia and fat body. Conversely, *upd3* overexpression mildly enhanced the response under conditions of sterile and septic injury (Fig. 7H), resembling the effect of *imd* overexpression (see Fig. 6H) and suggesting that *upd3* in hemocytes is required but not sufficient.

Since Upd3 is a ligand of the Jak/Stat pathway, we probed for the requirement of pathway components in the putatively receiving tissues. Indeed, RNAi silencing of *hopscotch* (*hop*) (*Drosophila* Jak) or *Stat92E* in the respiratory system partially reduced the overall *Drosocin* response (Fig. 7I, J). Likewise, silencing of *hop* or *Stat92E* in the fat body led to partial reduction in total *Drosocin* expression (Fig. 7K, L). This suggests that Jak/Stat signaling in both the respiratory epithelia and fat body are required to respond to hemocyte-expressed Upd3, and to contribute jointly to overall *Drosocin* expression, consistent with our earlier

findings. Unexpectedly, overexpression of activated Jak *hop*^{TumL} in fat body, or activated *Stat92E* (combined *Stat92E; Stat92E*$^{\Delta N \Delta C}$) in the respiratory system or fat body, reduced *Drosocin* levels after infection (Suppl. Fig. 6E–G). Crosses of *UAS-hop*^{TumL} with the tracheal driver *btl-GAL4* were largely lethal and gave rise to only a minimal number of escapers, despite the use of *tub-GAL80*^{ts} to avoid expression during development. The unexpected effects of Jak/Stat overexpression might be due to some unintended activation of a negative feedback loop or other complex secondary signaling changes.

Altogether, our findings suggest that hemocytes act as sentinels of bacterial infection, which signal to neighboring cells of the respiratory epithelia and fat body. Hemocyte-expressed *upd3* and Jak/Stat signaling in the respiratory epithelia and fat body are required, albeit not sufficient, in this process. In response, both fat body and respiratory epithelia concertedly contribute to the expression of *Drosocin*.

Drosocin expression in the respiratory epithelia and fat body promote animal survival after infection

Lastly, we asked whether *Drosocin* expression in the respiratory epithelia and fat body is crucial for animal survival after infection. First we determined whether ubiquitous RNAi silencing of *Drosocin* affects animal survival after immune challenge. Indeed survival after bacterial infection with gram-negative *E. coli* or *E. cloacae* was significantly reduced, an effect seen with two independent *Drosocin* RNAi lines (Fig. 8A,D). In some but not all experiments, *Drosocin* knockdown affected survival after PBS injection (Fig. 8B). Ubiquitous knockdown of *Drosocin* did not affect the induction of other AMPs following bacterial infection (Suppl.Fig. 7A–D), strengthening the idea that endogenous Drosocin has direct antibacterial role/s, and does not act as signal or mediator that would sustain the expression of other AMPs following bacterial infection.

Next we probed the role of *Drosocin* expression specifically in the blood cell reservoir. Indeed, *Drosocin* silencing in the respiratory system or fat body significantly reduced survival after *E. coli* infection (Fig. 8H,K), an effect that was seen with two independent *Drosocin* RNAi lines. *Drosocin* knockdown in either of the two tissues showed an occasional, partially penetrant effect on survival after PBS injection (Fig. 8I,L). As expected, silencing of *Drosocin* in hemocytes had no significant effect on survival following gram-negative infection or injury (Fig. 8E,F).

Taken together, we conclude that endogenous *Drosocin* expression in the respiratory system and fat body of adult *Drosophila* is effective in promoting animal survival after gram-negative infection, and suggest *Drosocin* expression may also contribute in some ways to survival after injury through PBS injection. This protective role of localized *Drosocin* expression is directly linked to the reservoir of blood cells and their function as sentinels of infection. By identifying Imd signaling and *upd3* expression in hemocytes as required initial step in this relay, our work establishes a *Drosophila* model to study multi-tissue organismal immunity.

Discussion

Adult *Drosophila* has been a powerful system to dissect molecular mechanisms underlying innate immunity, (Imler and Bulet, 2005; Lemaitre and Hoffmann, 2007; Morin-Poulard et al., 2013; Royet and Dziarski, 2007), but major questions have remained regarding the hematopoietic capacity of the *Drosophila* adult blood cell system, and the role of blood cells in organismal immunity. We discovered a central role for an extensive blood cell reservoir at the respiratory epithelia and fat body of adult *Drosophila*. The reservoir serves as major receptacle of blood cells and foreign particles, and in addition executes a local humoral immune response of *Drosocin* expression that promotes animal survival after bacterial infection. Both functions are tied together by hemocytes acting as sentinels of infection, that signal through the Imd pathway and Upd3 to induce the *Drosocin* in the tissues of their surrounding reservoir, i.e. the respiratory epithelia and colocalizing domains of the fat body.

Historic literature on *Drosophila* and other insects focused on the adult heart as the site of hemocyte accumulation. It described clusters of hemocytes at the ostia of the heart as “immune organ” (Gupta, 2009), locations where hemocytes and bacteria accumulate (King and Hillyer, 2012). More recently, adult blood cell production at the heart was proposed (Ghosh et al., 2015). Some studies described functions of hemocytes in other locations, such as at the ovaries or along the gut of adult flies (Ayyaz et al., 2015; Van De Bor et al., 2015). Taking a more global cryosectioning approach afforded us to identify the largest reservoir of hemocytes in adult *Drosophila*, which surrounds the respiratory epithelia and is lined by fat body of the thorax and head. We conclude that hemocytes and particles are delivered to these areas by the streaming hemolymph, even though the detailed anatomy of the open circulatory system remains to be mapped in more detail. Hemocytes may be physically caught in these locations, or in addition may engage in active adhesion. The intimate relationship of hemocytes with the respiratory epithelia, hemolymph, and adjacent fat body may serve interconnected roles, (1) guarding the respiratory epithelia as a barrier to the environment with respect to the roles of hemocytes in both phagocytosis and the induction of humoral immunity, and (2) facilitating gas exchange of hemocytes and nearby immune tissues, which in turn may again benefit defense functions. The former may be particularly advantageous in the defense against fungal pathogens that invade *Drosophila* via the tracheal system as primary route of infection, such as the entomopathogenic fungus *B. bassiana* (Clarkson and Charnley, 1996; Lemaitre et al., 1997). Regarding the latter, a study in caterpillars described the association of hemocytes with trachea, proposing a function for the respiratory system to supply hemocytes with oxygen (Locke, 1997).

Drosophila adult blood cells derive from two lineages: one that originates in the embryo and resembles vertebrate tissue macrophages, and another that produces blood cells in the lymph gland through a progenitor-based mechanism (Banerjee et al., 2019; Gold and Brückner, 2014, 2015; Holz et al., 2003) Our estimate that more than 60% of adult hemocytes derive from the embryonic lineage is surprising, considering past views that the majority of adult hemocytes would derive from the lymph gland (Lanot et al., 2001), It places more importance on the *Drosophila* embryonic lineage of hemocytes and suggest additional parallels with tissue macrophages in vertebrates, which persist into adulthood and form a separate myeloid system independent of the progenitor-derived monocyte lineage (Davies et

al., 2013; Gold and Brückner, 2014, 2015; Perdiguero et al., 2014; Sieweke and Allen, 2013). Future research will show whether the relative contribution of the two hemocyte lineages to the adult blood cell pool will be the same or different under conditions of stress and immune challenges.

Given that embryonic-lineage plasmatocytes are highly proliferative in the hematopoietic pockets of the larva, and lymph gland hemocyte progenitors and some lymph gland plasmatocytes proliferate during larval development (Evans et al., 2003; Jung et al., 2005; Letourneau et al., 2016), the absence of hemocyte proliferation in the adult may be surprising. Nevertheless, combining our broad evidence supporting lack of significant hematopoietic activity in adult *Drosophila*, and evidence that Srp in adult *Drosophila* is not a progenitor marker, our findings robustly contradict an adult hematopoiesis model proposed by (Ghosh et al., 2015). Our findings further reveal important differences to embryonic development, where Srp is required for the specification of undifferentiated prohemocytes (Rehorn et al., 1996). We show that during maturation of the adult animal, hemocytes relocate to the respiratory epithelia and the heart, upon completion of cytolysis of larval fat body cells (Nelliot et al., 2006), thereby refuting claims of new blood cell production at the heart (Ghosh et al., 2015). Similarly, we explain seemingly increased numbers of fluorescently labeled hemocytes following bacterial infection, being based the infection-induced upregulation of hemocyte-specific genes and their respective enhancers, used e.g. in the reporter *Hml*Δ*-GAL4>UAS-GFP*. Enhanced hemocyte expression of *Hml* and other hemocyte-specific markers post infection was described previously (De Gregorio et al., 2001; Franc et al., 1999).

Taken together, this broad evidence speaks to a lack of significant hematopoietic capacity of the blood cell system in adult *Drosophila*. Our findings are in agreement with other studies that have reported a lack of hemocyte proliferation in adult *Drosophila* (Lanot et al., 2001; Mackenzie et al., 2011; Woodcock et al., 2015), and functional immunosenescence in ageing flies (Felix et al., 2012; Mackenzie et al., 2011). Despite the scope of conditions tested, we cannot exclude the possibility that some other specific immune challenge or stress might exist that would be potent enough to trigger proliferation- or differentiation-based blood cell production in adult *Drosophila*. Likewise, we cannot exclude that adult *Drosophila* may possess small numbers of proliferation-competent progenitors that may have persisted e.g. from the lymph gland posterior lobes (Grigorian et al., 2011; Jung et al., 2005); such cells might give rise to new differentiated hemocytes, although according to our data they would remain insignificant in number.

Taking into account the short reproductive phase and relatively short life span of *Drosophila*, the adult fly may be sufficiently equipped with the pool of hemocytes that is produced in the embryo and larva. In fact, hemocytes do not seem essential for the immediate survival of adult flies: *Drosophila* ablated of hemocytes, and mutants devoid of hemocytes, survive to adulthood (Arefin et al., 2015; Braun et al., 1998; Charroux and Royet, 2009; Defaye et al., 2009) although they are more prone to, and succumb more rapidly to, infection (Arefin et al., 2015; Basset et al., 2000; Braun et al., 1998; Charroux and Royet, 2009; Defaye et al., 2009). We propose a model that places emphasis on larval development as the sensitive phase for the expansion and regulation of the adult blood cell pool (Gold and Brückner,

2015) (Fig. 5N). In the larva, hemocytes of both the embryonic- and lymph gland lineage integrate signals from a variety of internal and external stimuli to adapt to existing life conditions (Gold and Brückner, 2014, 2015; Shim, 2015).

Our work reveals a role for hemocytes in a local humoral immune response of the fat body and respiratory epithelia. Previous studies on hemocyte-ablated flies have reported increases in *Defensin* and *IM1* expression (Charroux and Royet, 2009; Defaye et al., 2009). In contrast, we find a positive role for hemocytes in the induction of *Drosocin* in tissues that form the hemocyte reservoir, i.e. the respiratory epithelia and fat body domains of the head and thorax. The concept of hemocytes promoting AMP expression in other tissues is well established (Agaisse et al., 2003; Basset et al., 2000; Chakrabarti et al., 2016; Yang et al., 2015). A role for AMP expression in surface epithelia that interface with the environment was reported by (Ferrandon et al., 1998), and *Drosocin* expression was described in embryonic and larval trachea and the abdominal tracheal trunks of adult *Drosophila*, albeit not in the respiratory epithelia (Akhouayri et al., 2011; Tan et al., 2014; Tzou et al., 2000).

In adult *Drosophila*, hemocytes tightly localize between the respiratory epithelia and fat body tissue that occupies the space toward to the cuticle exoskeleton. We propose that this close anatomical relationship facilitates rapid local signaling. Consistent with previous knowledge that *Drosocin* expression is lost in *imd* mutant backgrounds (Lemaitre PNAS 1995; Rahel et al. JBC 2004), we find that hemocyte-autonomous Imd signaling is required, albeit not sufficient, to trigger the infection-induced *Drosocin* response. Likewise, the Imd pathway upstream receptor *PGRP-LC* is required in hemocytes, suggesting that DAP-type peptidoglycan recognition and initiation of Imd signaling are a critical step in triggering the *Drosocin* response. Transcriptional induction of *upd3* by Imd signaling is supported by putative Rel binding sites identified in the *upd3* genomic region, two of which are even fully conserved across the seven examined *Drosophilids* including *Drosophila melanogaster* (Copley et al., 2007). Our data suggest roles for hemocyte-expressed *upd3*, and corresponding Jak/Stat signaling in cells of the fat body and respiratory system, all of which are required albeit not sufficient. Overactivation of the pathway paradoxically suppresses *Drosocin* expression, and expression of activated hop^{TumL} in trachea was even largely lethal despite our use of $tub\text{-}GAL80^{ts}$, possibly indicating leaky expression of the transgene. Overall, we can only speculate that the unexpected effects of Jak/Stat overactivation might be due to activation of some negative feedback loop or other complex signaling changes.

Several reports provide precedent for a role of hemocyte-expressed Upd3 in the induction of immune responses in other target tissues. Following septic injury, upregulation of *upd3* in hemocytes triggers induction of stress peptide genes of the *turandot* family including *totA* in fat body (Agaisse et al., 2003; Brun et al., 2006). Similarly, in response to injury, hemocyte-produced Upd3 induces Jak/Stat signaling in the fat body and gut (Chakrabarti et al., 2016). Under lipid-rich diet, *upd3* is induced in hemocytes, causing impaired glucose homeostasis and reduced lifespan in adult *Drosophila* (Woodcock et al., 2015). In the larva, hemocyte-derived Upd2 and −3 activate Jak/Stat signaling in muscle, which are required for the immune response against parasitic wasps (Yang et al., 2015). However, in the *Drosocin* response around the reservoir of hemocytes, our data predict that additional signal/s and/or signaling pathway/s are needed to initiate *Drosocin* expression and potentially restrict its

expression to defined fat body domains of the head and thorax. Additional events may include signaling through Toll or other signaling pathways in hemocytes and/or other tissues including the respiratory epithelia and fat body. Likewise, other types of signals may be required, such as reactive oxygen species (ROS) or nitric oxide (NO) which were reported to play roles in the relay of innate immune responses to infection and stress (Caceres et al., 2011; Di Cara et al., 2018; Eleftherianos et al., 2014; Myers et al., 2018; Wu et al., 2012), or non-peptide hormones including ecdysone, which confers competence in the embryonic tracheal *Drosocin* response to bacterial infection, and enhances humoral immunity under conditions of dehydration (Tan et al., 2014; Zheng et al., 2018). Lastly, there could be a requirement for additional processing to make bacterial ligands accessible for receptors in other tissues, as has been reported for Psidin, a lysosomal protein required in blood cells for degradation of engulfed bacteria and expression of *Defensin* in the fat body (Brennan et al., 2007), although this mechanism may not be universal in all systems (Nehme et al., 2007).

Our work reveals an active role of endogenous *Drosocin* expression in survival after bacterial infection. Since the cloning of *Drosocin* and its classification as inducible antibacterial peptide (Bulet et al., 1993), *Drosocin* has been studied for its transcriptional regulation (Charlet et al., 1996), illustrating its induction under a variety of bacterial and other immune challenges (Akbar et al., 2011; Akhouayri et al., 2011; Becker et al., 2010; Clark et al., 2013; Fernando et al., 2014; Gendrin et al., 2013; Lemaitre et al., 2012; Yagi et al., 2013). Drosocin structure and antimicrobial function have been studied in vitro (Ahn et al., 2011; Bikker et al., 2006; McManus et al., 1999; Otvos et al., 2000b), and by overexpression from transgenes in *Drosophila* (Loch et al., 2017; Tzou et al., 2002; Vonkavaara et al., 2013) and in heterologous vertebrate systems (Otvos et al., 2000a). Consistent with our findings, a recent study that examined new CRISPR-based *Drosocin* null mutants reached similar conclusions regarding the requirement of endogenous *Drosocin* expression for animal survival following *E. cloacae* infection (Hanson et al., 2019). However, this study did not address anatomical features of *Drosocin* expression, nor its unique path of induction. In addition to *Drosocin*'s role in animal survival after bacterial infection, our data suggest contribution of *Drosocin* to animal survival after injury through PBS injection. Injury has emerged as a factor that affects survival, a phenomenon for which the molecular mechanisms still remain to be determined (Chambers et al., 2014). Alternatively, considering that survival experiments are performed over two weeks or more, and the fly surface and living conditions are not sterile, we cannot rule out that PBS injections may have led to inadvertent infection with some low level contaminating microbes. A role for endogenous Drosocin levels in the antimicrobial response is strongly supported by independent data in the literature. Specifically, the minimum inhibitory concentration (MIC) of Drosocin against *E. coli* and *E. cloacae* was determined to be well within the range or below the endogenous concentration of Drosocin in the *Drosophila* hemolymph (MIC is 1 μM or 2μM for the glycosylated forms, and 8 or 10μM for the unglycosylated form, respectively (Bulet et al., 1996), compared to 40μM Drosocin in the *Drosophila* hemolymph (Uttenweiler-Joseph et al., 1998).

In conclusion, our study revokes the use of adult *Drosophila* as effective model to study hematopoiesis, and establishes it as promising system for organismal immunity centering on the immune signaling relay at the reservoir of blood cells. At the evolutionary level, this

model shows parallels with vertebrate immune cells of the lung and innate immune responses to bacterial infection (Byrne et al., 2015; Divangahi et al., 2015; Opitz et al., 2010). The *Drosophila* model opens countless avenues for exciting future research, e.g. to investigate additional molecular and cellular mechanisms in the immune signaling relay, the role and regulation of the system in the defense against pathogens that invade the trachea as natural route of infection, the use of the same axis by gram-positive or non-bacterial pathogens, and the induction of other AMPs and immune effector genes in the same axis of regulation.

STAR Methods

LEAD CONTACT AND MATERIALS AVAILABILITY

Further information and requests for resources and reagents should be directed to and will be fulfilled by the Lead Contact Katja Brückner (katja.brueckner@ucsf.edu). All materials that were newly generated for this study such as plasmids and fly lines are available from the Lead Contact upon request.

EXPERIMENTAL MODEL AND SUBJECT DETAILS

Drosophila* strains and fly husbandry—Canton S, w1118*, or *yw* were used as control strains to match the background of experiment crosses. Transgenic lines and mutants used are listed in the Table S1. Recombinant chromosomes and combinations of transgenes were generated by standard genetic techniques. Unless stated otherwise, all genetic crosses were kept at 25°C. Flies were raised on a standard dextrose cornmeal diet supplemented with dry yeast. Female flies were used for the majority of the experiments (qPCR, survival assays, lineage tracing, microparticle injection), unless indicated otherwise in the Figure Legends or Methods.

METHOD DETAILS

Hml Fucci transgenic lines—To generate *HmlΔFucci-G1-Orange* and *HmlΔFucciGreenS/G2/M-Green* constructs, Fucci cloning vectors (MBL laboratories, AM-V9014 and AM-V9001) were both digested with HindIII and BamHI in order to excise the insert Fucci fluorescence genes; *Fucci-G1 Orange* and *Fucci-S/G2/M Green*. A previously cloned *p-Red H-Stinger-HmlΔ-DsRed* plasmid (Clark et al., 2011) was digested with BamHI and SpeI in order to excise *DsRed* whilst leaving the *HmlΔ* promoter in place. T4 DNA polymerase was used o blunt the *p-Red H-Stinger-HmlΔ* vector and the *Fucci* DNA inserts. Vector and *Fucci* insert DNA were then digested again with BamHI for a sticky-blunt ligation (Takara Bio Inc -TaKaRa DNA Ligation Kit LONG). Cloning was done according to standard procedures. The separate *HmlΔFucci-G1-Orange* and *HmlΔFucciGreenS/G2/M-Green* constructs were injected into w^{1118} *Drosophila* embryos to generate transgenic lines (BestGene Inc.). Plasmid maps and more detailed cloning information are available upon request.

Flipout-LacZ lineage tracing—Flipout-lacZ lineage tracing was essentially done as described by (Weigmann and Cohen, 1999). Lineage tracing of embryonic hemocytes was described previously in (Makhijani et al., 2011). F1 progeny of the following cross were

used *tub-GAL80^{ts}; UAS-Flp x srphemo-GAL4, UAS-srcEGFP; Act>stop>nuc-lacZ*. To obtain specific lacZ labeling of embryonic hemocytes, expression of *srpHemo-GAL4* through *tub-GAL80^{ts}* was controlled by shifting 5 hour egg collections from 18°C to the permissive temperature of 31°C for 6 hours and then back to 18° C until pupal or adult stage. The no heat shock control was continuously maintained at of 18°C. For lineage tracing of embryonic-lineage hemocytes from the larva, F1 progeny of the following cross were used *Hml*Δ*-GAL4, UAS-GFP x UAS-Flp; tub-GAL80^{ts} / CyO wee p; act>stop>lacZnls*. Heat shock at 29°C was administered from 0–48h AEL, and animals were then maintained at 18°C for the remainder of their life. This time window was chosen to avoid labeling of lymph gland-lineage hemocytes that express the *Hml*Δ*-GAL4* driver from a later point during larval development. βGal positive hemocytes, relative to all Crq positive plasmatocytes, were determined by immunostaining of ex vivo released hemocytes at two points, (1) from 3rd instar larva before mobilization of differentiated lymph gland hemoytes takes place, and (2) from adult animals at 12 days post eclosure. The relative fraction of labeled hemocytes in the adult compared to the larva was calculated from the average and standard deviation from 16 adult females.

Fucci analysis and quantification of hemocytes—Fucci analysis, imaging and external hemocyte counts for Fig. 3D and 5C-F' were performed using a Leica SP5 confocal microscope. Flies were affixed dorsally to glass cover slips with superglue (Loctite) Sf435746 and imaged in vivo using 20x Dry NA 0.5 or 40x Oil NA 1.25 objectives. Cohorts of 15–21 flies per condition were imaged, and images were processed using Fiji and Imaris software. Cell counts were performed using the MATLAB spot detection function in Imaris, calculating the mean±SEM, and performing an unpaired t test to calculate statistical significance. For bacterial infections related to Fucci analyses and hemocyte counts, individual *E. coli*, *M. luteus*, or *E. cloacae* cultures were grown at 37°C overnight. The following morning, cultures were centrifuged at 4°C at 1600rpm for 10 minutes. Bacterial pellets were re-suspended in PBS to a final OD600 of 1. Injection was performed using a PicospritzerR III (Parker Hannifin), and the injection volume was calibrated to 50nl by injecting a drop into a plot of oil. Adult males 7 days post eclosion were used for injections of bacteria, sterile PBS, and non-injected controls.

Hemocyte MARCM—We developed Hemocyte MARCM as a derivation of the previously described MARCM (Lee and Luo, 1999), a labeling method based on mitotic recombination. The ubiquitous *tub-GAL4* driver was replaced with *Hml*Δ*-GAL4* to allow specific GFP labeling of all dividing cells that would ultimately show Hml+ plasmatocyte characteristics (Makhijani et al., 2011). Genotypes of F1 progeny were as follows: Hemocyte MARCM: *hsflp,UAS-CD8GFP/ +; Hml*Δ*-GAL4/ Hml*Δ*-GAL4, UAS-GFP; FRT82B, tub-GAL80/ FRT82B*. Control: *hsflp, UAS-CD8GFP/ +; Hml*Δ*-GAL4/ Hml*Δ*-GAL4, UAS-GFP; FRT82B, tub-GAL80/ +*. Various heat shock and incubation schemes were tested to optimize Hemocyte MARCM labeling, using 1–2 week old adult progeny. Heatshock was induced at 37°C for 1h 3 times/day for 3 days; 30°C continuously for 4 days; 32°C continuously for 4 days. Following heat shock schemes, flies were maintained at room temperature and observed under a fluorescence stereomicroscope for GFP labeled hemocytes. The control cross lacks one of the FRT82B chromosome and therefore does not allow Flp-induced

recombination to occur. Progeny from control crosses was also exposed to heat shock, allowing to observe non-specific GFP labeling due to heat shock conditions and imbalance of GAL4 and GAL80, and/or occasional random recombination events. Groups of 12–18 animals (equal mix of males and females) were examined per condition. For immune challenges, 4–6 days old flies were infected with a mixture of *E. coli* and *M. luteus*, by pricking flies in the thorax with a needle dipped in a bacterial pellet (mix of equal OD600 from overnight cultures of *E. coli* and *M. luteus*).

PermaTwin MARCM—For PermaTwin MARCM, genotypes were essentially as described in (Fernandez-Hernandez et al., 2013). F1 progeny of the following cross were used: *w; FRT40A, UAS-CD8-GFP, UAS-CD2-Mir/Cyo; actGAL4, UAS-flp/TM6B* x *w; FRT40A, UAS-CD2-RFP, UAS-GFP-Mir/Cyo; tub-GAL80^{ts}/TM6B*. Flies were raised at 18°C until adulthood to repress *flp* expression. Adult progeny of different ages (3–5 days and 2–3 weeks, n=12/age and induction condition) were examined. Animals were shifted to 29°C for varying time windows of 4 days, 8 days, 2 weeks, 3 weeks, respectively, and observed by live imaging for appearance of GFP and RFP labeled hemocytes; control tissues with labeled clones were dissected and observed in parallel. Adults were also dissected in PBS, to examine for hemocyte populations that might be attached to internal tissues. Negative control flies were maintained at 18°C continuously. In order to test the effect of immune challenge on hemocyte proliferation in adults, flies of the above age and genotypes were infected with either *E. coli* (OD 3) or *M.luteus* (OD 1.5 or 2) and observed 2–8 days post-infection.

Cryosectioning, head dissections—For cryosectioning, adult whole flies were embedded in OCT (Tissue-Tek) and snap frozen on dry ice with 95% ethanol. Cryosections of 55μM thickness were obtained using a cryostat (Leica CM3050 S or Leica CM1950). Tissue sections were placed on charged glass slides and fixed with 4% PFA in 2xPBS with 2x Complete protease inhibitor (Roche) for 10 min, followed by 2% PFA for 10 min, and permeabilized with 0.2% Triton-X100 for 15 min. Dissections of the respiratory epithelia (air sacs) of the head were done using forceps and a dissection well filled with PBS. Heads were detached from the rest of the body. By holding heads at the proboscis, the cuticle of the head was opened through the antennae first, progressively working toward the posterior, trying to avoid damage of the respiratory epithelia. Once the brains with the overlying respiratory air sacs were exposed, they were fixed with 4% PFA/PBS for 10 minutes, washed in PBS and processed for imaging. In both cryosections and dissections, hemocyte attachment to the respiratory epithelia is quite fragile. Accordingly, some hemocyte loss occurs in many preparations.

Immunohistochemistry and other staining methods—To analyze hemocytes ex vivo, hemocytes of single flies were released in 100μl of Schneider's medium (Gibco, Millipore) or PBS supplemented with Complete 2x (Roche) and proteinase inhibitor 4-(2-Aminoethyl)benzenesulfonyl fluoride hydrochloride AEBSF (Sigma); flies were dissected and hemocytes were scraped from all inside areas of the fly (head, thorax and abdomen).

For immunohistochemistry, antibodies used were goat anti-GFP (Rockland Immunochemicals, 1:2000), rabbit anti-βGal (Thermo, 1:1000), rabbit anti-DsRed

(Rockland Immunochemicals, 1:1000), mouse P1 (P1a+P1b) (Kurucz et al., 2007a) (kind gift of I. Ando, 1:10), anti-Crq (Franc et al., 1996) (kind gift of C. Kocks, 1:1000), anti-Srp (kind gift of A. Giangrande, 1:1000) and secondary antibodies conjugated to Alexa dyes (Molecular Probes, 1:500), fluorescently labeled phalloidin (Molecular Probes), DAPI (Sigma), DRAQ5 (ThermoFisher).

Fat body cells were labeled using OilRedO (37%) dissolved in triethyl phosphate (6ml triethyl phosphate and 4 ml water) for 30 min, followed by three to four washes with distilled water. Other stainings used fluorescent LipidTOX dyes (LifeTech), diluted in PBS.

Edu incorporation assays—To assess cell proliferation in adult hemocytes, adult F1 progeny of *yw* or *HmlΔ-GAL4, UAS-GFP x CantonS* were maintained for 14 days on fly food supplemented with a stock of 0.5 mg/ml EdU (Invitrogen) to a final concentration of 0.4mM EdU. Animals were immune challenged with bacterial infections both before or during EdU feedings. Various ages of adult animals (starting labeling at 0–1 week after eclosion) and crosses with other control lines (Oregon R, w1118 etc.) were examined. Hemocytes were released in multi-well dishes ex vivo and Click-IT EdU detection was performed according to the manufacturer's instructions (Invitrogen).

Microbead and bioparticle injections—For microbead injections, adult females aged 3 or 11 days after eclosure were injected with a suspension of fluorescent beads (FluoSpheres carboxylate-modified 0.2 μm; Life Technologies); 50–69 nl of a 1:10 dilution in PBS of was injected as described previously (Makhijani et al., 2011). Flies were incubated at 25°C for 30min-1h, followed by imaging, hemocyte releases or embedding for cryosectioning. For quantification of bead-positive hemocytes, images were taken with a Leica DMI4000B microscope followed by manual counting.

For bioparticle injections, adult females aged 6 to 11 days after eclosure were injected with fluorescent bioparticles (*E. coli* K-12 Strain Bioparticles TexasRed Conjugate; Invitrogen) or pH sensitive fluorescent bioparticles (pHrodo *E. coli* Bioparticles Conjugate for Phagocytosis; Invitrogen). Each fly was injected with 27.6–32.2 nl of bioparticles (1mg/100μl) and then incubated at 25° C for 4 hours before analysis. For ex vivo hemocyte analysis of differential body sections, flies were split into head, thorax, abdomen using a scalpel, individually placed into wells of 20 μl of PBS, and hemocytes were released from each section by poking and crushing. Hemocytes were imaged as described under Microscopy.

Microscopy—Fluorescence images were obtained on a Leica DMI4000 microscope. A Leica M205FA stereomicroscope with motorized stage and Leica LAS Montage module was used to live CO2-anesthetized flies or whole mount stainings. Immunostained adult cryosections and dissected preparations were imaged using a Leica SP5 confocal microscope.

Hemocyte quantification from adult flies—To determine hemocyte numbers by visualization of fluorescent reporter expressing hemocytes through the cuticle, the number of GFP labeled hemocytes in thorax, three legs and head of one side of the animal was counted

from montage images (described above) for 1, 7, 19, 24, 37 and 63 days old adults. For each time point, 4–10 males and 4–10 females were used to determine the mean value of number of hemocytes and standard deviation. For hemocyte quantification in the dorsal thorax/abdominal area in (Fig. 5C-F'), see 'Fucci analysis and quantification of hemocytes'. To determine total hemocyte numbers by release, single flies were CO2-anesthetized, and dissected in a glass well slide containing defined amount of 70μl of Schneider's *Drosophila* medium (Millipore). Under a fluorescence stereomicroscope, the head was removed and the ventral side of the head was carefully torn between the eyes, and subsequently pinched with forceps until all of the hemocytes were released. The empty head was then removed from the well. Next, the abdomen was torn open and, starting from the posterior end, squeezed and poked until the majority of hemocytes were released. The thorax was squeezed/crushed multiple times to release the remaining hemocytes. The carcass was transferred out of the well. 10μl of this hemocyte suspension was pipetted into a hemocytometer, and cells were counted under a fluorescence microscope. Cell numbers from four $1mm^2$ squares were averaged, and the total number of hemocytes per fly was calculated. A total of 10 females plus 2 males per time point were quantified which were processed in groups of 4 animals. Average number of hemocytes/fly from 12 animals and standard deviation were calculated for each time point.

Bacterial infection—Animals for hemocyte MARCM, PermaTwin MARCM or EdU based proliferation experiments and qPCR to detect AMP expression were immune challenged by either injection or feeding of bacterial strains as outlined below.

For injections, bacterial cultures were grown overnight in LB broth with suitable antibiotics. The following morning, a 1:20 culture dilution was incubated at 37°C for 3 hours, OD measured (NanoDrop 2000c spectrophotometer, Thermo Scientific) while typically <1, and the culture was spun down and the resulting pellet resuspended in PBS to achieve specific calculated ODs as summarized below. Bacterial strains (kind gifts from Bruno Lemaitre laboratory) and ODs were as follows; *Escherichia coli* OD 3 or 6 (see figure legends); *Micrococcus luteus* OD 1.5 or 2; *Erwinia carotovora carotovora 15* (Lemaitre et al., 1997) OD 1.5; *Enterobacter cloacae* (ß12, Jean Lambert(Lemaitre et al., 1997)) OD 2 or 4 (see figure legends). Bacterial suspension or control (sterile PBS) was injected into the thorax or abdomen of anesthetized females aged 5–7 days using a Nanoject II injector (Drummond Scientific Inc.) fitted with a pulled glass capillary, using volumes of 9.2nl to 27.6nl as indicated; experiments with *btl-GAL4* used 1–2 days old flies. Infected adults were incubated at 29°C, or as indicated. F1 crosses of transgenes regulated by the temperature-sensitive *tub-GAL80^{ts}* (McGuire et al., 2003) were initially maintained at 18°C, and then induced by shifting animals to 29°C, starting 24 hours before injection for crosses with *HmlΔ-GAL4, UAS-GFP; tub-GAL80^{ts}*, or 48 hours before injection for crosses with *btl-GAL4, UAS-GFP, tub-GAL80^{ts}*. Immune challenge by feeding of *S. marcescens* was performed as described previously (Nehme et al., 2007). *S. marcescens* grown overnight from a single colony inoculated into 5 ml LB broth with 50ug/ml ampicillin was diluted to OD600 of 0.1 in 10 ml of fly food. At least 10 adults per cohort were used.

qRT-PCR—Adult flies were frozen at −80°C after incubation at 29°C following injections (see figure legends for specific incubation times). Frozen flies were pestle-homogenized in TRIzol (Invitrogen), and RNA was isolated using Direct-zol RNA MiniPrep kit, following the manufacturer's instructions (Zymo). RNA was quantified and quality checked with a NanoDrop 2000c spectrophotometer (Thermo Scientific). 1 g of RNA was reverse transcribed using iScript cDNA synthesis kit (BioRad) and the resulting cDNA was diluted 1/10 for the qPCR. qPCR was run in a BioRad CFX96 Touch Real-Time PCR System, or ABI Viia7 Real-Time PCR System using the BioRad iTaq SYBR Green Supermix. For qPCR analysis of AMPs, total RNA was harvested from 10 pooled adult female *Drosophila* for each experimental condition. For qPCR on split fly samples, 8 pooled females for each condition were snap frozen in LN2, and for each fly the head/thorax and abdomen were separated using a scalpel on a metal block on dry ice. Relative mRNA expression levels were normalized to that of *RpL32*. Primers used for qPCR are summarized in Table S1. Statistical analysis was performed as indicated in figure legends.

QUANTIFICATION AND STATISTICAL ANALYSIS

Image analysis was performed using Fiji (Schindelin et al., 2012) and Imaris (Oxford Instruments) software, as described in specific Methods Details sections. Prism 8 (Graphpad) and Excel (Microsoft Office) were used for statistical analysis and graphical representations. Sample sizes n of experiments are indicated in the Method Details section and Figure Legends. Experiments were repeated three times, and as indicated in the figure legends. We calculated the mean −/+ standard deviation or standard error of the mean, and performed significance testing by two-tailed t test or two-way ANOVA with Sidak's multiple comparison test as indicated in the Methods Details sections and Figure Legends.

DATA AND CODE AVAILABILITY

This study did not generate or analyze any large datasets or code.

Supplementary Material

Refer to Web version on PubMed Central for supplementary material.

Acknowledgements

We thank I. Ando, U. Banerjee, E. Bach, N. Buchon, M. Crozatier, J.P. Dudzic, C. Evans, A. Giangrande, L. Kockel, C. Kocks, T. Kornberg, M. Meister, P. Rao, B. Stramer, S. Younger, the Bloomington Stock Center, the DGRC and the VDRC for fly stocks and antibodies. We especially thank Prashanth Rao and Chrysoula Pitsouli for their expert advice on the *Drosophila* tracheal system and respiratory epithelia, and Mark Krasnow for expert advice on insect literature. Thanks to Jordan Augsburger for help with the Methods section, and members of the Brückner lab for feedback on the manuscript. KSG was supported by an American Heart Association fellowship. KM was supported by a Human Frontier Science Program long-term fellowship. PSB was supported by a Swiss National Science Foundation early postdoc mobility fellowship. K. J Woodcock and F. Geissmann were supported by a Wellcome Trust Senior Investigator Award (WT101853/C/13/Z) to FG. This work was supported by grants from the American Cancer Society RSG DDC-122595, American Heart Association 13BGIA13730001, National Science Foundation 1326268, National Institutes of Health 1R01GM112083-01, 1R56HL118726-01A1, and 1R01GM131094-01A1 (to KB). This investigation was in part conducted in a facility constructed with support from the Research Facilities Improvement Program, Grant number C06-RR16490 from the NCRR/NIH. Special thanks from KB to Steep Ravine Cabins at Mt. Tam State Park, CA.

References

Agaisse H, Petersen UM, Boutros M, Mathey-Prevot B, and Perrimon N (2003). Signaling Role of Hemocytes in *Drosophila* JAK/STAT-Dependent Response to Septic Injury. Dev Cell 5, 441–450. [PubMed: 12967563]

Ahn M, Murugan RN, Nan YH, Cheong C, Sohn H, Kim EH, Hwang E, Ryu EK, Kang SW, Shin SY, et al. (2011). Substitution of the GalNAc-alpha-O-Thr(1)(1) residue in drosocin with O-linked glyco-peptoid residue: effect on antibacterial activity and conformational change. Bioorg Med Chem Lett 21, 6148–6153. [PubMed: 21890357]

Akbar MA, Tracy C, Kahr WH, and Kramer H (2011). The full-of-bacteria gene is required for phagosome maturation during immune defense in *Drosophila*. J Cell Biol 192, 383–390. [PubMed: 21282466]

Akhouayri I, Turc C, Royet J, and Charroux B (2011). Toll-8/Tollo negatively regulates antimicrobial response in the *Drosophila* respiratory epithelium. PLoS Pathog 7, e1002319. [PubMed: 22022271]

Arefin B, Kucerova L, Krautz R, Kranenburg H, Parvin F, and Theopold U (2015). Apoptosis in Hemocytes Induces a Shift in Effector Mechanisms in the *Drosophila* Immune System and Leads to a Pro-Inflammatory State. PLoS One 10, e0136593. [PubMed: 26322507]

Ayyaz A, Li H, and Jasper H (2015). Haemocytes control stem cell activity in the *Drosophila* intestine. Nat Cell Biol 17, 736–748. [PubMed: 26005834]

Banerjee U, Girard JR, Goins LM, and Spratford CM (2019). *Drosophila* as a Genetic Model for Hematopoiesis. Genetics 211, 367–417. [PubMed: 30733377]

Basset A, Khush RS, Braun A, Gardan L, Boccard F, Hoffmann JA, and Lemaitre B (2000). The phytopathogenic bacteria Erwinia carotovora infects *Drosophila* and activates an immune response. Proc Natl Acad Sci U S A 97, 3376–3381. [PubMed: 10725405]

Becker T, Loch G, Beyer M, Zinke I, Aschenbrenner AC, Carrera P, Inhester T, Schultze JL, and Hoch M (2010). FOXO-dependent regulation of innate immune homeostasis. Nature 463, 369–373. [PubMed: 20090753]

Bergmann A, Agapite J, McCall K, and Steller H (1998). The *Drosophila* gene hid is a direct molecular target of Ras-dependent survival signaling. Cell 95, 331–341. [PubMed: 9814704]

Beutler BA (2009). TLRs and innate immunity. Blood 113, 1399–1407. [PubMed: 18757776]

Bikker FJ, Kaman-van Zanten WE, de Vries-van de Ruit AM, Voskamp-Visser I, van Hooft PA, Mars-Groenendijk RH, de Visser PC, and Noort D (2006). Evaluation of the antibacterial spectrum of drosocin analogues. Chem Biol Drug Des 68, 148–153. [PubMed: 17062012]

Braun A, Hoffmann JA, and Meister M (1998). Analysis of the *Drosophila* host defense in domino mutant larvae, which are devoid of hemocytes. Proc Natl Acad Sci U S A 95, 14337–14342. [PubMed: 9826701]

Brennan CA, Delaney JR, Schneider DS, and Anderson KV (2007). Psidin is required in *Drosophila* blood cells for both phagocytic degradation and immune activation of the fat body. Curr Biol 17, 67–72. [PubMed: 17208189]

Bretscher AJ, Honti V, Binggeli O, Burri O, Poidevin M, Kurucz E, Zsamboki J, Ando I, and Lemaitre B (2015). The Nimrod transmembrane receptor Eater is required for hemocyte attachment to the sessile compartment in *Drosophila melanogaster*. Biol Open 4, 355–363. [PubMed: 25681394]

Brückner K, Kockel L, Duchek P, Luque CM, Rørth P, and Perrimon N (2004). The PDGF/VEGF Receptor controls blood cell survival in *Drosophila*. Dev Cell 7.

Brun S, Vidal S, Spellman P, Takahashi K, Tricoire H, and Lemaitre B (2006). The MAPKKK Mekk1 regulates the expression of Turandot stress genes in response to septic injury in *Drosophila*. Genes Cells 11, 397–407. [PubMed: 16611243]

Bulet P, Dimarcq JL, Hetru C, Lagueux M, Charlet M, Hegy G, Van Dorsselaer A, and Hoffmann JA (1993). A novel inducible antibacterial peptide of *Drosophila* carries an O-glycosylated substitution. J Biol Chem 268, 14893–14897. [PubMed: 8325867]

Bulet P, Urge L, Ohresser S, Hetru C, and Otvos L Jr. (1996). Enlarged scale chemical synthesis and range of activity of drosocin, an O-glycosylated antibacterial peptide of *Drosophila*. European journal of biochemistry 238, 64–69. [PubMed: 8665953]

Byrne AJ, Mathie SA, Gregory LG, and Lloyd CM (2015). Pulmonary macrophages: key players in the innate defence of the airways. Thorax 70, 1189–1196. [PubMed: 26286722]

Caceres L, Necakov AS, Schwartz C, Kimber S, Roberts IJ, and Krause HM (2011). Nitric oxide coordinates metabolism, growth, and development via the nuclear receptor E75. Genes Dev 25, 1476–1485. [PubMed: 21715559]

Chakrabarti S, Dudzic JP, Li X, Collas EJ, Boquete JP, and Lemaitre B (2016). Remote Control of Intestinal Stem Cell Activity by Haemocytes in *Drosophila*. PLoS Genet 12, e1006089. [PubMed: 27231872]

Chambers MC, Jacobson E, Khalil S, and Lazzaro BP (2014). Thorax injury lowers resistance to infection in *Drosophila melanogaster*. Infect Immun 82, 4380–4389. [PubMed: 25092914]

Charlet M, Lagueux M, Reichhart JM, Hoffmann D, Braun A, and Meister M (1996). Cloning of the gene encoding the antibacterial peptide drosocin involved in *Drosophila* immunity. Expression studies during the immune response. European journal of biochemistry 241, 699–706. [PubMed: 8944755]

Charroux B, and Royet J (2009). Elimination of plasmatocytes by targeted apoptosis reveals their role in multiple aspects of the *Drosophila* immune response. Proc Natl Acad Sci U S A 106, 9797–9802. [PubMed: 19482944]

Clark RI, Tan SW, Pean CB, Roostalu U, Vivancos V, Bronda K, Pilatova M, Fu J, Walker DW, Berdeaux R, et al. (2013). MEF2 is an in vivo immune-metabolic switch. Cell 155, 435–447. [PubMed: 24075010]

Clark RI, Woodcock KJ, Geissmann F, Trouillet C, and Dionne MS (2011). Multiple TGF-beta superfamily signals modulate the adult *Drosophila* immune response. Curr Biol 21, 1672–1677. [PubMed: 21962711]

Clarkson JM, and Charnley AK (1996). New insights into the mechanisms of fungal pathogenesis in insects. Trends Microbiol 4, 197–203. [PubMed: 8727600]

Copley RR, Totrov M, Linnell J, Field S, Ragoussis J, and Udalova IA (2007). Functional conservation of Rel binding sites in drosophilid genomes. Genome Res 17, 1327–1335. [PubMed: 17785540]

Davies LC, Jenkins SJ, Allen JE, and Taylor PR (2013). Tissue-resident macrophages. Nat Immunol 14, 986–995. [PubMed: 24048120]

De Gregorio E, Spellman PT, Rubin GM, and Lemaitre B (2001). Genome-wide analysis of the *Drosophila* immune response by using oligonucleotide microarrays. Proc Natl Acad Sci U S A 98, 12590–12595. [PubMed: 11606746]

De Gregorio E, Spellman PT, Tzou P, Rubin GM, and Lemaitre B (2002). The Toll and Imd pathways are the major regulators of the immune response in *Drosophila*. Embo J 21, 2568–2579. [PubMed: 12032070]

Defaye A, Evans I, Crozatier M, Wood W, Lemaitre B, and Leulier F (2009). Genetic ablation of *Drosophila* phagocytes reveals their contribution to both development and resistance to bacterial infection. J Innate Immun 1, 322–334. [PubMed: 20375589]

Di Cara F, Sheshachalam A, Braverman NE, Rachubinski RA, and Simmonds AJ (2018). Peroxisome-Mediated Metabolism Is Required for Immune Response to Microbial Infection. Immunity 48, 832–833. [PubMed: 29669255]

Dionne MS, Ghori N, and Schneider DS (2003). *Drosophila melanogaster* is a genetically tractable model host for Mycobacterium marinum. Infect Immun 71, 3540–3550. [PubMed: 12761139]

Divangahi M, King IL, and Pernet E (2015). Alveolar macrophages and type I IFN in airway homeostasis and immunity. Trends Immunol 36, 307–314. [PubMed: 25843635]

Ekas LA, Cardozo TJ, Flaherty MS, McMillan EA, Gonsalves FC, and Bach EA (2010). Characterization of a dominant-active STAT that promotes tumorigenesis in *Drosophila*. Dev Biol 344, 621–636. [PubMed: 20501334]

Eleftherianos I, More K, Spivack S, Paulin E, Khojandi A, and Shukla S (2014). Nitric oxide levels regulate the immune response of *Drosophila melanogaster* reference laboratory strains to bacterial infections. Infect Immun 82, 4169–4181. [PubMed: 25047850]

Elrod-Erickson M, Mishra S, and Schneider D (2000). Interactions between the cellular and humoral immune responses in *Drosophila*. Curr Biol 10, 781–784. [PubMed: 10898983]

Evans CJ, Hartenstein V, and Banerjee U (2003). Thicker than blood: conserved mechanisms in *Drosophila* and vertebrate hematopoiesis. Dev Cell 5, 673–690. [PubMed: 14602069]

Felix TM, Hughes KA, Stone EA, Drnevich JM, and Leips J (2012). Age-specific variation in immune response in *Drosophila melanogaster* has a genetic basis. Genetics 191, 989–1002. [PubMed: 22554890]

Fernandez-Hernandez I, Rhiner C, and Moreno E (2013). Adult neurogenesis in Drosophila. Cell Rep 3, 1857–1865. [PubMed: 23791523]

Fernando MD, Kounatidis I, and Ligoxygakis P (2014). Loss of Trabid, a new negative regulator of the *Drosophila* immune-deficiency pathway at the level of TAK1, reduces life span. PLoS Genet 10, e1004117. [PubMed: 24586180]

Ferrandon D, Jung AC, Criqui M, Lemaitre B, Uttenweiler-Joseph S, Michaut L, Reichhart J, and Hoffmann JA (1998). A drosomycin-GFP reporter transgene reveals a local immune response in *Drosophila* that is not dependent on the Toll pathway. Embo J 17, 1217–1227. [PubMed: 9482719]

Franc NC, Dimarcq JL, Lagueux M, Hoffmann J, and Ezekowitz RA (1996). Croquemort, a novel *Drosophila* hemocyte/macrophage receptor that recognizes apoptotic cells. Immunity 4, 431–443. [PubMed: 8630729]

Franc NC, Heitzler P, Ezekowitz RA, and White K (1999). Requirement for croquemort in phagocytosis of apoptotic cells in *Drosophila*. Science 284, 1991–1994. [PubMed: 10373118]

Gendrin M, Zaidman-Remy A, Broderick NA, Paredes J, Poidevin M, Roussel A, and Lemaitre B (2013). Functional analysis of PGRP-LA in *Drosophila* immunity. PLoS One 8, e69742. [PubMed: 23922788]

Georgel P, Naitza S, Kappler C, Ferrandon D, Zachary D, Swimmer C, Kopczynski C, Duyk G, Reichhart JM, and Hoffmann JA (2001). *Drosophila* immune deficiency (IMD) is a death domain protein that activates antibacterial defense and can promote apoptosis. Dev Cell 1, 503–514. [PubMed: 11703941]

Ghosh S, Singh A, Mandal S, and Mandal L (2015). Active hematopoietic hubs in *Drosophila* adults generate hemocytes and contribute to immune response. Dev Cell 33, 478–488. [PubMed: 25959225]

Gold KS, and Brückner K (2014). *Drosophila* as a model for the two myeloid blood cell systems in vertebrates. Exp Hematol 42, 717–727. [PubMed: 24946019]

Gold KS, and Brückner K (2015). Macrophages and cellular immunity in *Drosophila melanogaster*. Semin Immunol 27, 357–368. [PubMed: 27117654]

Grigorian M, Mandal L, and Hartenstein V (2011). Hematopoiesis at the onset of metamorphosis: terminal differentiation and dissociation of the *Drosophila* lymph gland. Dev Genes Evol 221, 121–131. [PubMed: 21509534]

Guha A, and Kornberg TB (2005). Tracheal branch repopulation precedes induction of the *Drosophila* dorsal air sac primordium. Dev Biol 287, 192–200. [PubMed: 16198330]

Gupta AP (2009). Insect Hemocytes. Cambridge University Press.

Hanson MA, Dostalova A, Ceroni C, Poidevin M, Kondo S, and Lemaitre B (2019). Synergy and remarkable specificity of antimicrobial peptides in vivo using a systematic knockout approach. Elife 8.

Harrison DA, Binari R, Nahreini TS, Gilman M, and Perrimon N (1995). Activation of a Drosophila Janus kinase (JAK) causes hematopoietic neoplasia and developmental defects. Embo J 14, 2857–2865. [PubMed: 7796812]

Holz A, Bossinger B, Strasser T, Janning W, and Klapper R (2003). The two origins of hemocytes in *Drosophila*. Development 130, 4955–4962. [PubMed: 12930778]

Imler JL, and Bulet P (2005). Antimicrobial peptides in *Drosophila*: structures, activities and gene regulation. Chem Immunol Allergy 86, 1–21. [PubMed: 15976485]

Jung SH, Evans CJ, Uemura C, and Banerjee U (2005). The *Drosophila* lymph gland as a developmental model of hematopoiesis. Development 132, 2521–2533. [PubMed: 15857916]

Kaneko T, Yano T, Aggarwal K, Lim JH, Ueda K, Oshima Y, Peach C, Erturk-Hasdemir D, Goldman WE, Oh BH, et al. (2006). PGRP-LC and PGRP-LE have essential yet distinct functions in the *Drosophila* immune response to monomeric DAP-type peptidoglycan. Nat Immunol 7, 715–723. [PubMed: 16767093]

Kim JY, Jang W, Lee HW, Park E, and Kim C (2012). Neurodegeneration of *Drosophila* drop-dead mutants is associated with hypoxia in the brain. Genes Brain Behav 11, 177–184. [PubMed: 22010830]

King JG, and Hillyer JF (2012). Infection-induced interaction between the mosquito circulatory and immune systems. PLoS Pathog 8, e1003058. [PubMed: 23209421]

Kopp EB, and Medzhitov R (1999). The Toll-receptor family and control of innate immunity. Curr Opin Immunol 11, 13–18. [PubMed: 10047546]

Kurucz E, Markus R, Zsamboki J, Folkl-Medzihradszky K, Darula Z, Vilmos P, Udvardy A, Krausz I, Lukacsovich T, Gateff E, et al. (2007a). Nimrod, a putative phagocytosis receptor with EGF repeats in *Drosophila* plasmatocytes. Curr Biol 17, 649–654. [PubMed: 17363253]

Kurucz E, Vaczi B, Markus R, Laurinyecz B, Vilmos P, Zsamboki J, Csorba K, Gateff E, Hultmark D, and Ando I (2007b). Definition of *Drosophila* hemocyte subsets by cell-type specific antigens. Acta Biol Hung 58 Suppl, 95–111. [PubMed: 18297797]

Lanot R, Zachary D, Holder F, and Meister M (2001). Postembryonic hematopoiesis in *Drosophila*. Dev Biol 230, 243–257. [PubMed: 11161576]

Lee T, and Luo L (1999). Mosaic analysis with a repressible cell marker for studies of gene function in neuronal morphogenesis. Neuron 22, 451–461. [PubMed: 10197526]

Leitao AB, and Sucena E (2015). *Drosophila* sessile hemocyte clusters are true hematopoietic tissues that regulate larval blood cell differentiation. Elife.

Lemaitre B, and Hoffmann J (2007). The host defense of *Drosophila melanogaster*. Annu Rev Immunol 25, 697–743. [PubMed: 17201680]

Lemaitre B, Nicolas E, Michaut L, Reichhart JM, and Hoffmann JA (2012). Pillars article: the dorsoventral regulatory gene cassette spatzle/Toll/cactus controls the potent antifungal response in *Drosophila* adults. Cell. 1996 86: 973–983. J Immunol 188, 5210–5220.

Lemaitre B, Reichhart JM, and Hoffmann JA (1997). *Drosophila* host defense: differential induction of antimicrobial peptide genes after infection by various classes of microorganisms. Proc Natl Acad Sci U S A 94, 14614–14619. [PubMed: 9405661]

Letourneau M, Lapraz F, Sharma A, Vanzo N, Waltzer L, and Crozatier M (2016). *Drosophila* hematopoiesis under normal conditions and in response to immune stress. FEBS Lett 590, 4034–4051. [PubMed: 27455465]

Leulier F, Parquet C, Pili-Floury S, Ryu JH, Caroff M, Lee WJ, Mengin-Lecreulx D, and Lemaitre B (2003). The *Drosophila* immune system detects bacteria through specific peptidoglycan recognition. Nat Immunol 4, 478–484. [PubMed: 12692550]

Loch G, Zinke I, Mori T, Carrera P, Schroer J, Takeyama H, and Hoch M (2017). Antimicrobial peptides extend lifespan in *Drosophila*. PLoS One 12, e0176689. [PubMed: 28520752]

Locke M (1997). Caterpillars have evolved lungs for hemocyte gas exchange. J Insect Physiol 44, 1–20. [PubMed: 12770439]

Mackenzie DK, Bussiere LF, and Tinsley MC (2011). Senescence of the cellular immune response in *Drosophila melanogaster*. Exp Gerontol 46, 853–859. [PubMed: 21798332]

Makhijani K, Alexander B, Tanaka T, Rulifson E, and Brückner K (2011). The peripheral nervous system supports blood cell homing and survival in the *Drosophila* larva. Development 138, 5379–5391. [PubMed: 22071105]

Makhijani K, and Brückner K (2012). Of blood cells and the nervous system: Hematopoiesis in the *Drosophila* larva. Fly (Austin) 6, 254–260. [PubMed: 23022764]

Manning G, and Krasnow MA (1993). Development of the *Drosophila* tracheal system In The Development of *Drosophila melanogaster*, Cold Spring Harbor Laboratory Press.

Markus R, Laurinyecz B, Kurucz E, Honti V, Bajusz I, Sipos B, Somogyi K, Kronhamn J, Hultmark D, and Ando I (2009). Sessile hemocytes as a hematopoietic compartment in *Drosophila melanogaster*. Proc Natl Acad Sci U S A 106, 4805–4809. [PubMed: 19261847]

McGuire SE, Le PT, Osborn AJ, Matsumoto K, and Davis RL (2003). Spatiotemporal rescue of memory dysfunction in *Drosophila*. Science 302, 1765–1768. [PubMed: 14657498]

McManus AM, Otvos L Jr., Hoffmann R, and Craik DJ (1999). Conformational studies by NMR of the antimicrobial peptide, drosocin, and its non-glycosylated derivative: effects of glycosylation on solution conformation. Biochemistry 38, 705–714. [PubMed: 9888811]

Morin-Poulard I, Vincent A, and Crozatier M (2013). The *Drosophila* JAK-STAT pathway in blood cell formation and immunity. Jakstat 2, e25700. [PubMed: 24069567]

Myers AL, Harris CM, Choe KM, and Brennan CA (2018). Inflammatory production of reactive oxygen species by *Drosophila* hemocytes activates cellular immune defenses. Biochem Biophys Res Commun 505, 726–732. [PubMed: 30292413]

Nehme NT, Liegeois S, Kele B, Giammarinaro P, Pradel E, Hoffmann JA, Ewbank JJ, and Ferrandon D (2007). A model of bacterial intestinal infections in *Drosophila melanogaster*. PLoS Pathog 3, e173. [PubMed: 18039029]

Nelliot A, Bond N, and Hoshizaki DK (2006). Fat-body remodeling in *Drosophila melanogaster*. Genesis 44, 396–400. [PubMed: 16868920]

Opitz B, van Laak V, Eitel J, and Suttorp N (2010). Innate immune recognition in infectious and noninfectious diseases of the lung. Am J Respir Crit Care Med 181, 1294–1309. [PubMed: 20167850]

Otvos L Jr., Bokonyi K, Varga I, Otvos BI, Hoffmann R, Ertl HC, Wade JD, McManus AM, Craik DJ, and Bulet P (2000a). Insect peptides with improved protease-resistance protect mice against bacterial infection. Protein Sci 9, 742–749. [PubMed: 10794416]

Otvos L Jr., O I, Rogers ME, Consolvo PJ, Condie BA, Lovas S, Bulet P, and Blaszczyk-Thurin M (2000b). Interaction between heat shock proteins and antimicrobial peptides. Biochemistry 39, 14150–14159. [PubMed: 11087363]

Perdiguero EG, Klapproth K, Schulz C, Busch K, Azzoni E, Crozet L, Garner H, Trouillet C, de Bruijn MF, Geissmann F, et al. (2014). Tissue-resident macrophages originate from yolk-sac-derived erythro-myeloid progenitors. Nature.

Rao PR, Lin L, Huang H, Guha A, Roy S, and Kornberg TB (2015). Developmental compartments in the larval trachea of Drosophila. Elife 4.

Rehorn KP, Thelen H, Michelson AM, and Reuter R (1996). A molecular aspect of hematopoiesis and endoderm development common to vertebrates and *Drosophila*. Development 122, 4023–4031. [PubMed: 9012522]

Royet J, and Dziarski R (2007). Peptidoglycan recognition proteins: pleiotropic sensors and effectors of antimicrobial defences. Nat Rev Microbiol 5, 264–277. [PubMed: 17363965]

Schindelin J, Arganda-Carreras I, Frise E, Kaynig V, Longair M, Pietzsch T, Preibisch S, Rueden C, Saalfeld S, Schmid B, et al. (2012). Fiji: an open-source platform for biological-image analysis. Nat Methods 9, 676–682. [PubMed: 22743772]

Shim J (2015). *Drosophila* blood as a model system for stress sensing mechanisms. BMB Rep 48, 223–228. [PubMed: 25560697]

Sieweke MH, and Allen JE (2013). Beyond stem cells: self-renewal of differentiated macrophages. Science 342, 1242974. [PubMed: 24264994]

Sinenko SA, and Mathey-Prevot B (2004). Increased expression of *Drosophila* tetraspanin, Tsp68C, suppresses the abnormal proliferation of ytr-deficient and Ras/Raf-activated hemocytes. Oncogene 23, 9120–9128. [PubMed: 15480416]

Song W, Onishi M, Jan LY, and Jan YN (2007). Peripheral multidendritic sensory neurons are necessary for rhythmic locomotion behavior in *Drosophila* larvae. Proc Natl Acad Sci U S A 104, 5199–5204. [PubMed: 17360325]

Takeda K, and Akira S (2005). Toll-like receptors in innate immunity. Int Immunol 17, 1–14. [PubMed: 15585605]

Tan KL, Vlisidou I, and Wood W (2014). Ecdysone mediates the development of immunity in the *Drosophila* embryo. Curr Biol 24, 1145–1152. [PubMed: 24794300]

Tzou P, De Gregorio E, and Lemaitre B (2002). How *Drosophila* combats microbial infection: a model to study innate immunity and host-pathogen interactions. Curr Opin Microbiol 5, 102–110. [PubMed: 11834378]

Tzou P, Ohresser S, Ferrandon D, Capovilla M, Reichhart JM, Lemaitre B, Hoffmann JA, and Imler JL (2000). Tissue-specific inducible expression of antimicrobial peptide genes in *Drosophila* surface epithelia. Immunity 13, 737–748. [PubMed: 11114385]

Uttenweiler-Joseph S, Moniatte M, Lagueux M, Van Dorsselaer A, Hoffmann JA, and Bulet P (1998). Differential display of peptides induced during the immune response of *Drosophila*: a matrix-

assisted laser desorption ionization time-of-flight mass spectrometry study. Proc Natl Acad Sci U S A 95, 11342–11347. [PubMed: 9736738]

Van De Bor V, Zimniak G, Papone L, Cerezo D, Malbouyres M, Juan T, Ruggiero F, and Noselli S (2015). Companion Blood Cells Control Ovarian Stem Cell Niche Microenvironment and Homeostasis. Cell Rep 13, 546–560. [PubMed: 26456819]

von Trotha JW, Egger B, and Brand AH (2009). Cell proliferation in the *Drosophila* adult brain revealed by clonal analysis and bromodeoxyuridine labelling. Neural Dev 4, 9. [PubMed: 19254370]

Vonkavaara M, Pavel ST, Holzl K, Nordfelth R, Sjostedt A, and Stoven S (2013). Francisella is sensitive to insect antimicrobial peptides. J Innate Immun 5, 50–59. [PubMed: 23037919]

Weigmann K, and Cohen SM (1999). Lineage-tracing cells born in different domains along the PD axis of the developing *Drosophila* leg. Development 126, 3823–3830. [PubMed: 10433911]

White K, Tahaoglu E, and Steller H (1996). Cell killing by the *Drosophila* gene reaper. Science 271, 805–807. [PubMed: 8628996]

Whitten JM (1957). The post-embryonic development of the tracheal system in *Drosophila melanogaster*. J Cell Sci *s3* 98, 123–150.

Woodcock KJ, Kierdorf K, Pouchelon CA, Vivancos V, Dionne MS, and Geissmann F (2015). Macrophage-derived upd3 cytokine causes impaired glucose homeostasis and reduced lifespan in *Drosophila* fed a lipid-rich diet. Immunity 42, 133–144. [PubMed: 25601202]

Wu SC, Liao CW, Pan RL, and Juang JL (2012). Infection-induced intestinal oxidative stress triggers organ-to-organ immunological communication in *Drosophila*. Cell Host Microbe 11, 410–417. [PubMed: 22520468]

Yagi Y, Lim YM, Tsuda L, and Nishida Y (2013). fat facets induces polyubiquitination of Imd and inhibits the innate immune response in *Drosophila*. Genes Cells 18, 934–945. [PubMed: 23919485]

Yang H, Kronhamn J, Ekstrom JO, Korkut GG, and Hultmark D (2015). JAK/STAT signaling in *Drosophila* muscles controls the cellular immune response against parasitoid infection. EMBO Rep 16, 1664–1672. [PubMed: 26412855]

Zasloff M (2002). Antimicrobial peptides of multicellular organisms. Nature 415, 389–395. [PubMed: 11807545]

Zheng W, Rus F, Hernandez A, Kang P, Goldman W, Silverman N, and Tatar M (2018). Dehydration triggers ecdysone-mediated recognition-protein priming and elevated antibacterial immune responses in *Drosophila* Malpighian tubule renal cells. BMC Biol 16, 60. [PubMed: 29855367]

Zhou L, Hashimi H, Schwartz LM, and Nambu JR (1995). Programmed cell death in the *Drosophila* central nervous system midline. Curr Biol 5, 784–790. [PubMed: 7583125]

Highlights

- Adult *Drosophila* have an extensive blood cell reservoir at the respiratory epithelia
- No sign of hematopoiesis in adult *Drosophila*, even after bacterial infection
- Blood cells act as sentinels of infection, via PGRP-LC/Imd/Upd3 signaling
- In tissues of the reservoir this induces *Drosocin* expression to promote survival

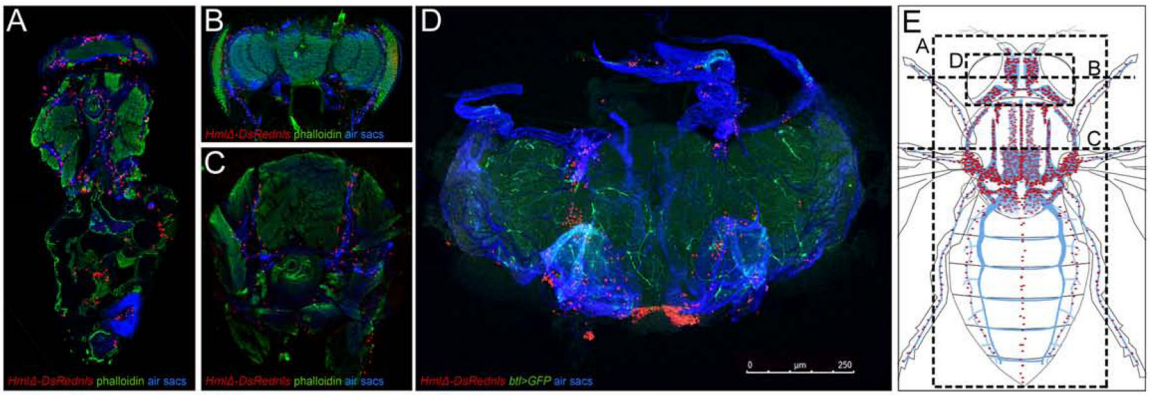

Figure 1. The respiratory epithelia provide the largest reservoir of hemocytes in adult *Drosophila*.

(A-C) Cryosections of adult *Drosophila*, *Hml*Δ-*DsRednls* hemocytes red, phalloidin green, respiratory epithelia (air sacs) blue. (A) Longitudinal section, anterior up; (B) cross section of head, dorsal up; (C) cross section of thorax, dorsal up. (D) Adult *Drosophila*, genotype *Hml*Δ-*DsRed*/+; *btl-GAL4, UAS-GFP*/+ ; hemocytes red, tracheal marker green; respiratory epithelia (air sacs) blue; dissection of head, anterior up; size bar 250µm. (E) Schematics of the the tracheal system and respiratory epithelia of the thorax and head (blue), hemocytes in red. Dashed lines indicate sections and dissected area shown in A-D. Note that model omits heart area, which is not visible in longitudinal section in (A). For full model, see Suppl. Fig. 1.

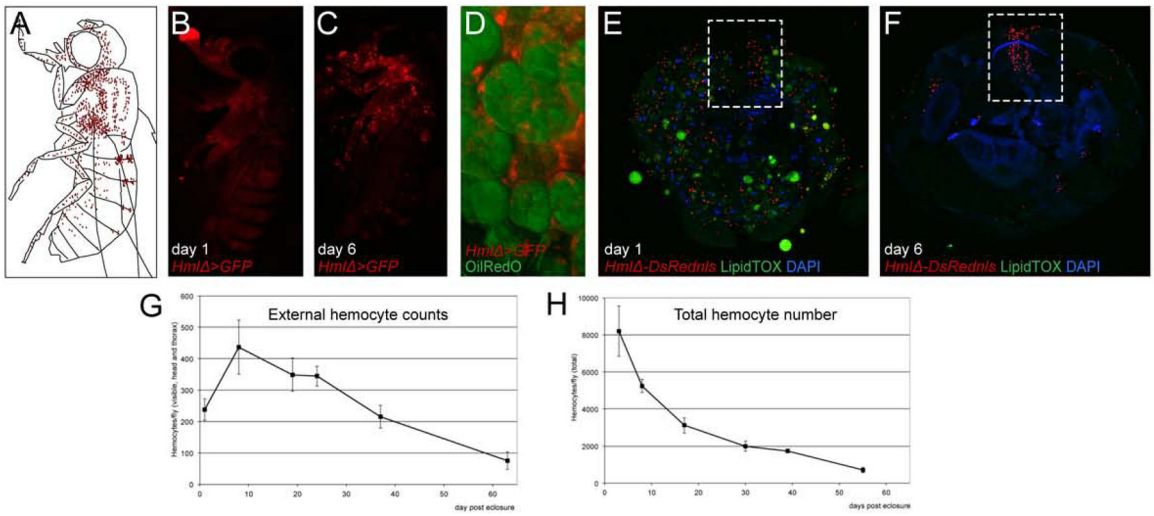

Figure 2. Developmental changes of hemocytes.

(A-C) Lateral view of adult *Drosophila*, (A) Model, hemocytes red, (B,C) *Hml*Δ-*GAL4, UAS-GFP* (hemocytes, red pseudo color), (B) day 1 post eclosure, (C) day 6 post eclosure. (D) Larval fat body cells (Oil Red O pseudo-colored green) with associated hemocytes (*Hml*Δ-*GAL4, UAS-GFP* pseudo-colored red), dissection of abdomen. (E, F) cross sections of anterior abdomen, *Hml*Δ-*DsRednls* (hemocytes red), LipidTox (green), DAPI (blue); dashed box marks heart region; (E) day 1 post eclosure; (F) day 6 post eclosure. (G) External hemocyte quantification of fluorescently labeled hemocytes, time course. (H) Total hemocyte counts per animal, time course.

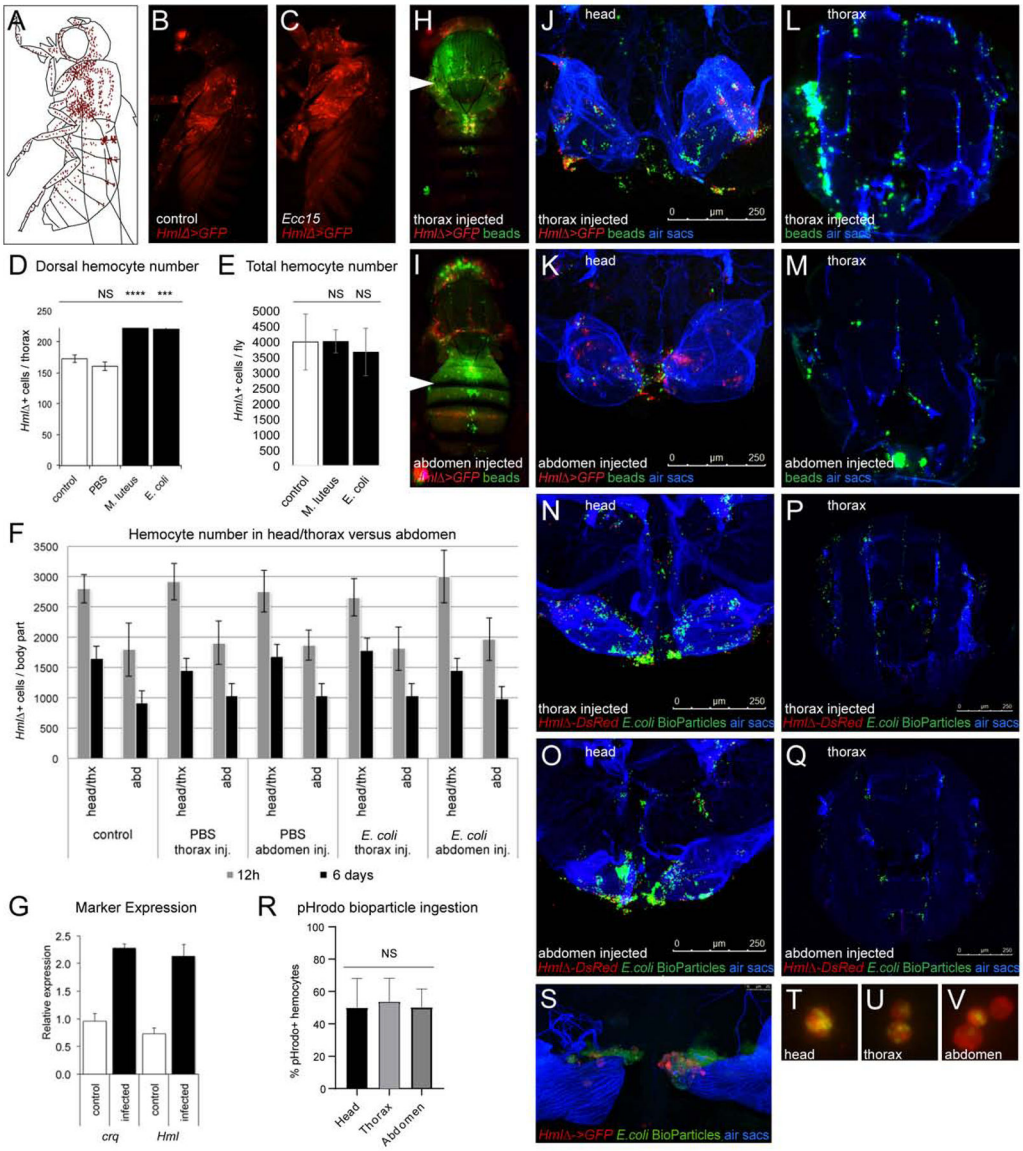

Figure 3. Infection-induced changes of hemocytes and accumulation of particles at the respiratory epithelia.

(A-C) Lateral view of adult *Drosophila*; (A) Model, hemocytes red, (B, C) *Hml*Δ-*GAL4, UAS-GFP* (hemocytes red pseudo color), (B) no infection control, (C) *Ecc15* injection. (D) External hemocyte quantification, dorsal thorax and anterior abdomen, controls and injected flies; p values of paired 2-tailed t test, *,**,***,or **** corresponding to p≤0.05, 0.01, 0.001, or 0.0001. (E) Total hemocyte counts, control and injected flies. Average and standard deviation; 2-tailed t test shows no statistically significant difference (NS). (F) Total hemocyte counts of flies split in two parts, head and thorax versus abdomen; control and injected flies. Flies were injected into thorax or abdomen at 5 days post eclosion and assayed at 12h and 6d post injection. Average and standard deviation. (G) qPCR expression levels of *Hml* and *Crq* from whole flies, −/+ infection, 48h post infection. 8 day old adults injected with *E.coli* at OD 2. (H-M) Injection of fluorescent microbeads (green pseudo color), *Hml*Δ-*GAL4, UAS-GFP* (hemocytes, red pseudo color), respiratory epithelia (air sacs, blue). (H, J,

L) Injection in thorax, (H) external view, (J) head dissection, (L) thorax cross section. (I, K, M) Injection in abdomen, (I) external view, (K) head dissection, (M) thorax cross section. (N-Q) Injection of fluorescent *E. coli* bioparticles (green), *Hml*Δ-*DsRed* for head dissections or *Hml*Δ-*DsRednls* for cryosections (hemocytes, red), respiratory epithelia (air sacs, blue). (N, P) Injection in thorax, (N) head dissection, (P) thorax cross section. (O, Q) Injection in abdomen, (O) head dissection, (Q) thorax cross section. (R) Injection of pHrodo *E. coli* bioparticles into *Hml*Δ-*DsRed* adults; % of hemocytes positive for pHrodo bioparticles from head, thorax and abdomen 4 h post injection. Mean and standard deviation; one-way ANOVA shows no statistically significant difference (NS). (S) Dissected respiratory epithelia of the head from adults *Hml*Δ-*DsRed* (hemocytes, red) injected with pHrodo *E. coli* bioparticles (green) 4 hours post injection. (T-V) Examples of hemocytes with incorporated pHrodo bioparticles isolated from head, thorax, abdomen, corresponding to (R).

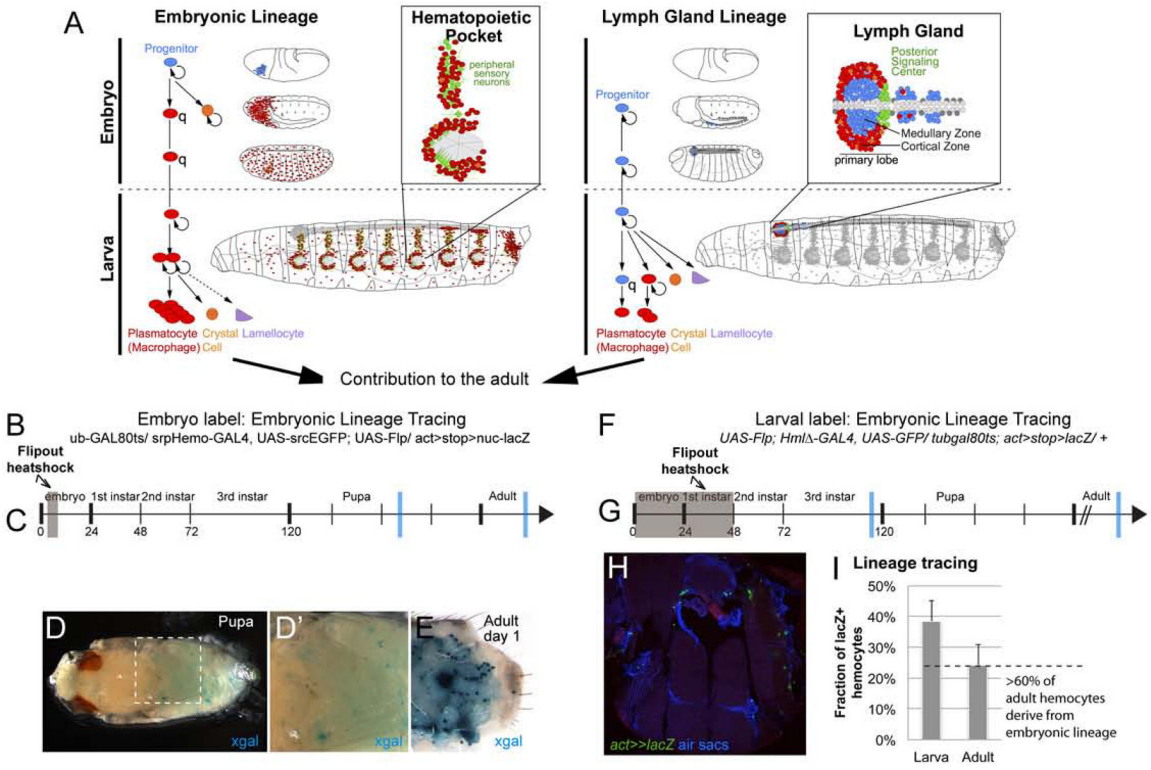

Figure 4. Contribution of the two hemocyte lineages to the adult blood cell pool.

(A) Timeline of the embryonic and lymph gland lineage, with major sites of hematopoiesis in the larva (hematopoietic pockets and lymph gland). Both lineages persist into the adult. (B-E) *flipout-lacZ* lineage tracing using *srpHemo-GAL4*. (B) Experimental genotype *tub-GAL80^{ts} / srpHemo-GAL4, UAS-srcEGFP; UAS-Flp/ act>stop>nuc-lacZ*. (C) Timeline of induction, hemocytes of the embryo were labeled in a 6h time window of Flp expression (grey box); blue bars mark time points of samples in (D-E). (D-D') *lacZ*/βGal positive hemocytes in the pupa, x-gal staining (blue); (E) *lacZ*/βGal positive hemocytes in the dissected adult abdomen, x-gal staining (blue); note occasional labeling of larval fat body cells. (F-I) *flipout-lacZ* lineage tracing, *HmlΔ-GAL4*. (F) Experimental genotype *UAS-Flp; HmlΔ-GAL4, UAS-GFP/ tub-GAL80^{ts}; act>stop>lacZ/ +*. (G) timeline, induction at 0–48h AEL (grey box). Note that at this stage lymph gland hemocytes do not express *HmlΔ-GAL4*. Blue bars mark time points of samples examined and quantified in (H, I); (H) Thorax cross section of adult fly, genotype as in (F), *lacZ*/βGal positive hemocytes green (anti-βGal), air sacs and DAPI blue. (I) Fraction of *lacZ*/βGal positive hemocytes relative to all Crq positive hemocytes in late 3rd instar larvae, and in the adult; ratio suggest contribution of the embryonic lineage to the adult blood cell pool (dashed line).

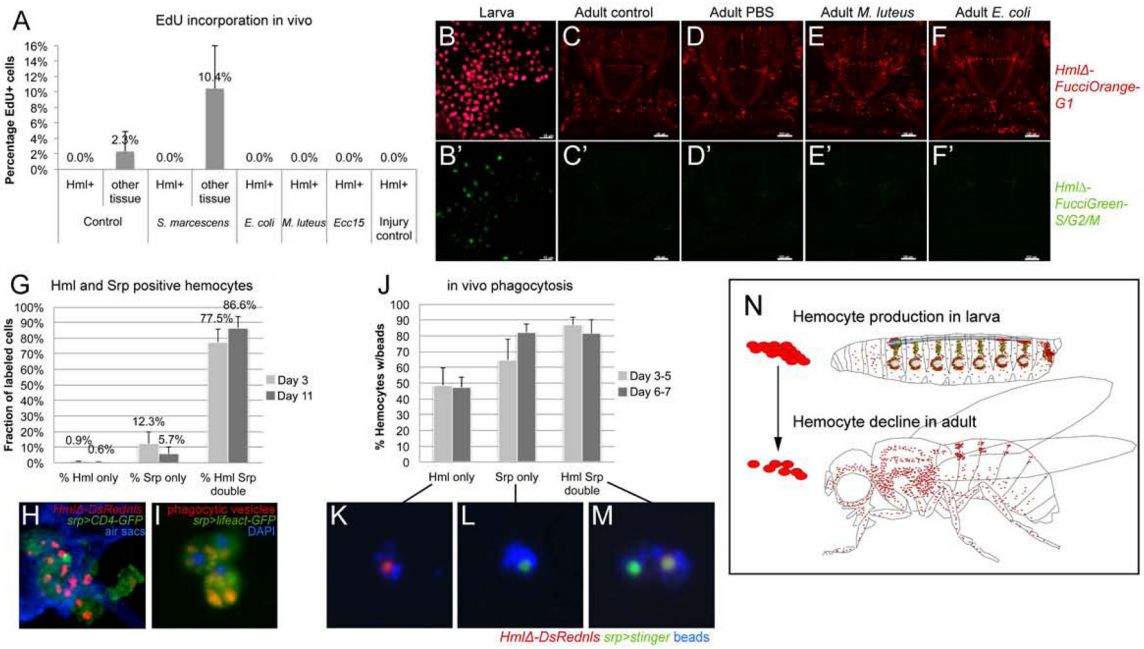

Figure 5. Adult hemocytes do not expand; Srp marks active phagocytes in adult *Drosophila*.

(A) In vivo EdU incorporation. Percentage of EdU positive cells among hemocytes or control tissue in absence or presence of immune challenges as indicated; average and standard deviation. (B-F') 2-color Fucci analysis of hemocytes, control (uninfected), sterile injury (PBS), and infection (*M. luteus*, *E. coli*); genotype is w^{1118}; *HmlΔFucciOrange*^{G1}; *HmlΔFucciGreen*$^{G2/S/M}$; (B-B') embryonic-lineage hemocytes released from larvae, note green cells; (C-F') imaging of Fucci hemocytes in adult flies, dorsal views of thorax and anterior abdomen, anterior up; note absence of green signal of *HmlΔFucciGreen*$^{G2/S/M}$. (G-I) *Srp* labels phagocytic plasmatocytes in the adult fly. (G) *Srp* and *Hml* positive hemocytes, young (3 days) and mature (11 days) adults.. (H) Thorax cross section of adult fly, genotype is *HmlΔDsrednls/UAS-CD4-GFP; +/srpD-GAL4;* respiratory epithelia (air sacs, blue). (I) *Srp-Gal4, UAS-lifeact-GFP* positive plasmatocytes (green) with red phagocytic vesicles, released ex vivo from adult fly; DAPI (blue). (J-M) In vivo phagocytosis assay, ex vivo examination of hemocytes. (J) % of hemocytes carrying blue beads, from young (3 days) and mature (11 days) adults. Genotype is *HmlΔDsred/ UAS-stinger; +/ srpD-GAL4*. (K, L, M) examples of labeled hemocytes as indicated. (N) Model, hemocyte production takes place during the larval stage (mainly in the hematopoietic pockets and the lymph gland), while in the adult hemocyte numbers decline over time.

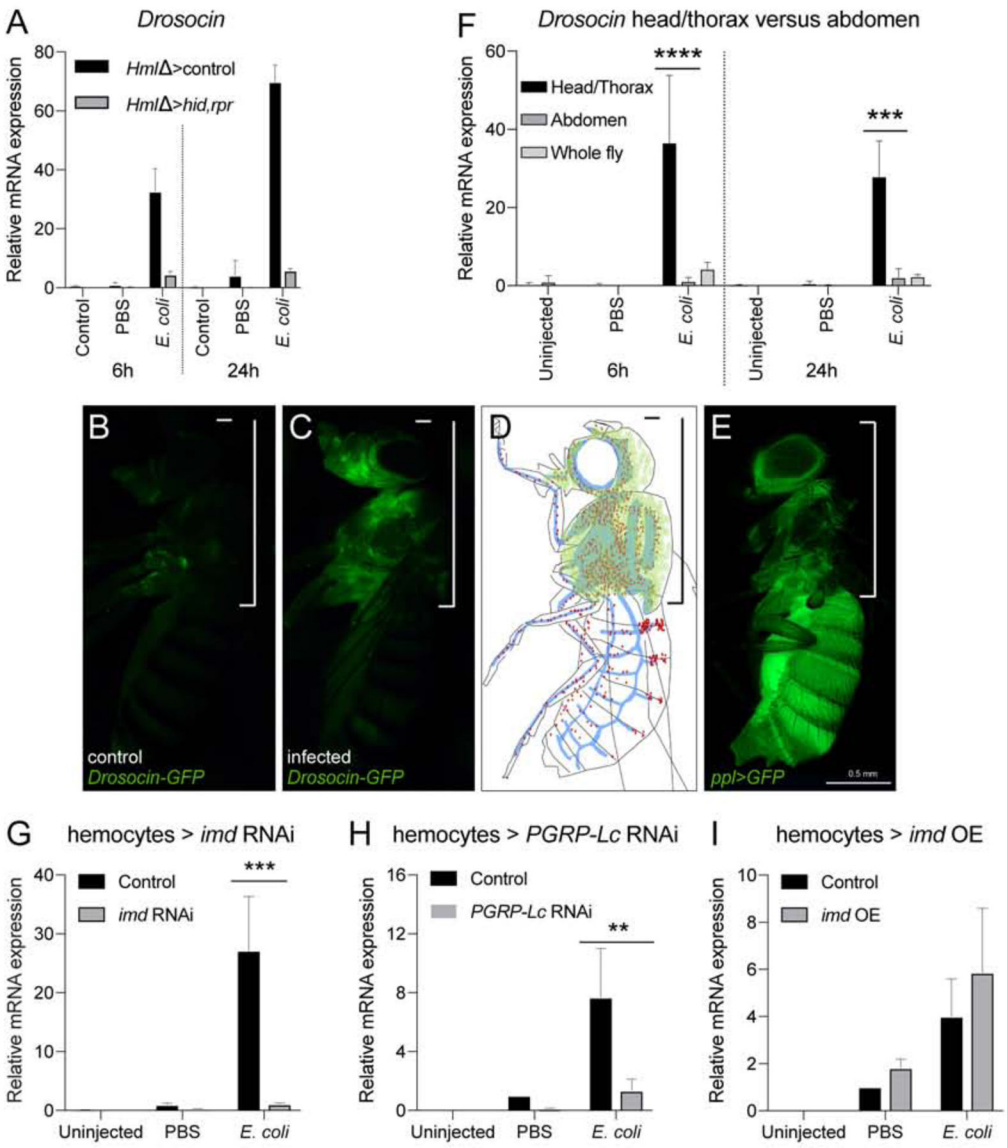

Figure 6. Hemocytes and Imd signaling are required for the induction of antimicrobial peptide genes including *Drosocin*.

(A) Expression of *Drosocin* in hemocyte-ablated flies and controls. 5 day-old adult *Drosophila* untreated, injected with sterile PBS, or with *E.coli* in PBS (OD 6), 9.2 nl; genotypes are *HmlΔ-GAL4, UAS-GFP/+* (control) or *w; HmlΔ-GAL4, UAS-GFP/ UAS-rpr; UAS-hid/+* (hemocyte ablation); flies harvested at 6h and 24h post injection. Chart displays mean and standard error of the mean (SEM) of samples from a representative biological replicate experiment, using pools of 10 females per condition, and triplicate qPCR runs. Values are displayed relative to the RNA level induced by the sterile PBS injections in control flies. (B-D) *Drosocin-GFP* expression is restricted to the head and thorax. (B) *Dro-GFP* uninfected control; (C) *Dro-GFP* infected; (D) model of *Dro-GFP* expression (green), hemocytes (red), tracheal system (blue). (E) Location of fat body throughout the animal marked by *ppl-GAL4, UAS-GFP* (green). (F) *Drosocin* qPCR of head/thorax versus abdomen tissue. Flies were left untreated, or injected with sterile PBS, or *E.coli* in PBS (OD

6), 9.2 nl, and harvested at 6 and 24h post infection. Two-way ANOVA with Sidak's multiple comparison test, *,**,***,or **** corresponding to p≤ 0.05, 0.01, 0.001, or 0.0001, respectively. (G-I) Expression of *Drosocin* in adult flies upon manipulation of Imd pathway activity. 5 day-old adult *Drosophila* untreated, injected with sterile PBS, or with *E.coli* in PBS (OD 6), 9.2 nl; flies harvested at 6h post injection. Charts display mean and confidence interval (CI) of samples from 3 averaged biological replicate experiments, using pools of 10 females per condition, and triplicate qPCR runs for each sample. Values of all charts are displayed relative to the average RNA level induced by the sterile PBS injections in control flies. Two-way ANOVA with Sidak's multiple comparison test, *,**,***,or **** corresponding to p≤0.05, 0.01, 0.001, or 0.0001, respectively. Transgenes were inducibly expressed in hemocytes 24 hours before injections. (G) *Drosocin* RNA levels of control (*HmlΔ-GAL4,UAS-GFP/+; tub-GAL80^{ts}/+*) versus *HmlΔ-GAL4,UAS-GFP/+; tub-GAL80^{ts}/UAS-imd RNAi*; (H) control versus *HmlΔ-GAL4,UAS-GFP/+; tub-GAL80^{ts}/UAS-PGRP-LC RNAi*; (I) control versus *HmlΔ-GAL4,UAS-GFP/UAS-imd; tub-GAL80^{ts}/+*.

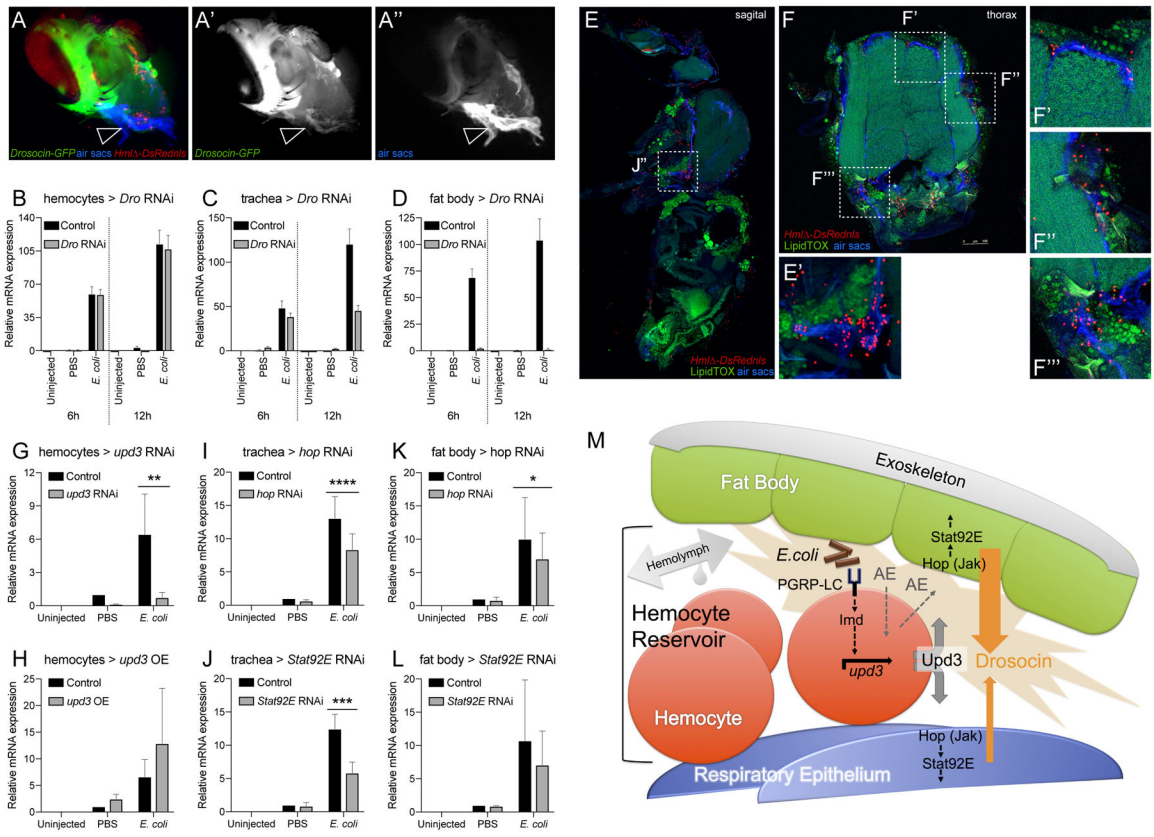

Figure 7. The *Drosocin* response is localized to the reservoir of hemocytes at the respiratory epithelia and colocalizing fat body domains, and requires Upd3 signaling from hemocytes.

(A-A”) Dissected heads of genotype *Drosocin-GFP/Hml*Δ*-DsRed* (Drosocin-GFP green, hemocytes red), respiratory epithelia (air sacs, blue); (A’) Drosocin-GFP, white; (A”) respiratory epithelia, white. Note *Drosocin-GFP* expression is high in fat body and moderate in respiratory epithelia (arrowhead). (B-D) Tissue specific RNAi knockdown of *Drosocin*; overall *Drosocin* mRNA levels were quantified by qPCR. 6–7 day-old adult females were left untreated, injected with PBS, or *E.coli* in PBS (OD 6), 9.2 nl, and harvested 6 and 12h post infection. Charts display mean and SEM of samples from a representative biological replicate experiment, using pools of 10 females per condition, and triplicate qPCR runs. Values of all charts are displayed relative to the RNA level induced by the sterile PBS injections in control flies. (B) *Drosocin* RNAi silencing in hemocytes; (C) in respiratory system; (D) in fat body. (E-F’’’) Anatomy of fat body tissue lining the respiratory epithelia and hemocytes; *Hml*Δ*-DsRednls* (hemocytes, red), fat body (LipidTOX, large, distinct green cells), respiratory epithelia (air sacs, blue) (E) Sagital section of adult *Drosophila*. (E’) Closeup of region indicated in (E). (F) Thorax cross section. (F’-F’’’) Closeup of regions indicated in (F). (G-L) Expression of *Drosocin* in adult flies upon silencing or overexpression of *upd3* and silencing of genes of the Jak/Stat pathway. 5 day-old adult *Drosophila* untreated, injected with sterile PBS, or *E.coli* in PBS (OD 6), 9.2 nl; flies harvested at 6h post injection. Charts display mean and CI of samples from 3 averaged biological replicate experiments, using pools of 10 females per condition, and triplicate qPCR runs for each sample. Values of all charts are displayed relative to the average RNA

level induced by the sterile PBS injections in control flies. Two-way ANOVA with Sidak's multiple comparison test, *,**,***,or **** corresponding to p≤0.05, 0.01, 0.001, or 0.0001, respectively. (G, H) *Drosocin* qPCR of whole flies, inducible transgene expression in hemocytes, (G) Genotypes are control (*HmlΔ-GAL4,UAS-GFP/+; tub-GAL80^{ts}* /+) versus *HmlΔ-GAL4,UAS-GFP/+; tub-GAL80^{ts} /UAS-upd3* RNAi. (H) Control versus *HmlΔ-GAL4,UAS-GFP/ UAS-upd3; tub-GAL80^{ts}* /+. (I, J) *Drosocin* qPCR of whole flies, inducible transgene expression in tracheal system. (I) Genotypes are control *(btl-GAL4, tub-GAL80^{ts}*, *UAS-GFP* /+) versus *btl-GAL4, tub-GAL80^{ts}, UAS-GFP / UAS-hop* RNAi; (J) Genotypes are control versus *btl-GAL4, tub-GAL80^{ts}, UAS-GFP / UAS-Stat92E* RNAi. (K, L) *Drosocin* qPCR of whole flies, transgene expression in fat body. (K) Genotypes are control (*ppl-GAL4, UAS-GFP* / +) versus *ppl-GAL4, UAS-GFP* /+; *UAS-hop* RNAi/+; (L) Genotypes are control versus *ppl-GAL4, UAS-GFP*/+; *UAS-Stat92E* RNAi/+. (M) Model of communication between hemocytes, fat body and respiratory epithelia, in which hemocytes act as sentinels of infection. Gram-negative bacteria that accumulate together with hemocytes in the reservoir between respiratory epithelia and fat body; activation of Imd signaling through PGRP-LC on hemocytes triggers *upd3* expression and Upd3 secretion. Upd3 activates Jak/Stat signaling in adjacent domains of the fat body and the respiratory epithelia, contributing directly or indirectly to the induction of *Drosocin* expression. Since we PGRP-LC/Imd signaling and Upd3/Jak/Stat signaling are required but not sufficient to induce *Drosocin* expression, additional events (AE) in parallel to these pathways are proposed that would provide sufficiency to trigger *Drosocin* induction.

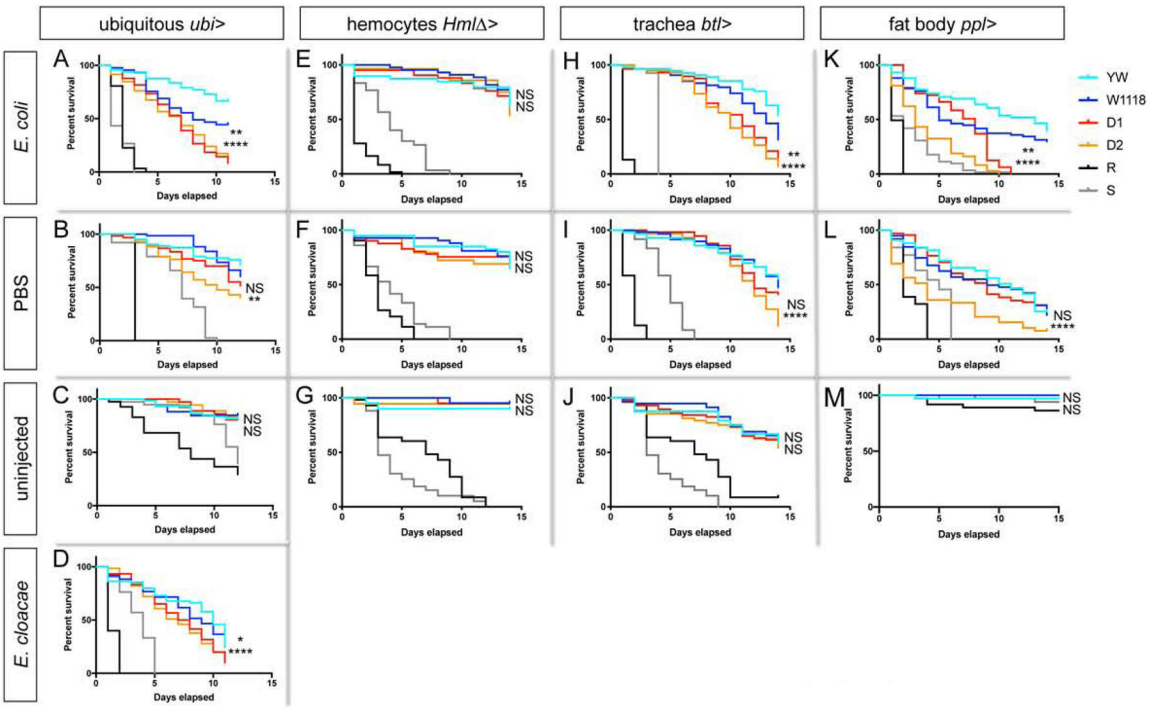

Figure 8. *Drosocin* silencing in respiratory epithelia and fat body decreases animal survival after infection.

(A-D) Survival assays. Adult female F1 progeny from crosses of GAL4 drivers with the following lines: *UAS-Drosocin RNAi* lines (D1, D2) or controls (*yw* (YW), w^{1118} (W1118)). Mutant Rel^{E20} (R) and spz^{rm7} (S) as controls. Figure displays one out of 3 comparable biological replicate experiments; in each experiment, for each genotype and condition 40 to 60 females were assessed; p-values log-rank (Mantel-Cox) test, *,**,***,or **** corresponding to p≤0.05, 0.01, 0.001, or 0.0001, respectively; upper symbol for comparison *w1118* vs. *Dro* RNAi D1; lower symbol for comparison of crosses of *yw* vs. *Dro* RNAi D2. 5 day old female flies were treated as follows and then incubated at 29°C. (A-D) *Ubi-GAL4* crosses, (A) *E. coli* (OD6, 9.2 nl); (B) sterile PBS injection (9.2nl); (C) uninjected control; (D) *E. cloacae* (OD4, 9.2nl). (E-G) *HmlΔ-GAL4* crosses, (E) *E. coli* (OD6, 9.2 nl); (F) sterile PBS injection (9.2nl); (G) uninjected control. (H-J) *btl-GAL4* crosses, (H) *E. coli* (OD6, 9.2 nl); (I) sterile PBS injection (9.2nl); (J) uninjected control. (K-M) *ppl-GAL4* crosses, (K) *E. coli* (OD6, 9.2 nl); (L) sterile PBS injection (9.2nl); (M) uninjected control. *Drosocin* knockdown with ubiquitous driver, or tracheal system- or fat body driver caused significantly reduced survival after gram-negative infection in all replicates. *Drosocin* knockdown showed a partially penetrant effect on survival after PBS injection: Tracheal system knockdown: survival significantly reduced for D1 in 0 out of 3 replicate experiments, for D2 in 2 out of 3 replicate experiments. Fat body knockdown: survival significantly reduced for D1 in 1 out of 3 replicate experiments, for D2 in 1 out of 3 replicate experiments. Ubiquitous *Drosocin* knockdown: survival was significantly reduced for D1 in 2 out of 3 replicate experiments, for D2 in 3 out of 3 replicate experiments. As expected, survival was not affected when *Drosocin* was silenced in hemocytes (E, F, G).

KEY RESOURCES TABLE

REAGENT or RESOURCE	SOURCE	IDENTIFIER
Antibodies		
goat anti-GFP	Rockland Immunochemicals	600-101-215
rabbit anti-βGal	Thermo	PI31887
rabbit anti-DsRed	Rockland Immunochemicals	600-401-379
mouse P1 (P1a+P1b)	From I. Ando lab (Kurucz et al., 2007b)	N/A
rabbit anti-Crq	From C. Kocks (Franc et al., 1996)	N/A
rabbit anti-Srp	A. Giangrande	N/A
donkey anti-goat Alexa 488	Molecular probes	A-11055
donkey anti-rabbit Alexa 488	Molecular probes	A-21206
donkey anti-mouse Alexa 488	Molecular probes	A-21202
Bacterial and Virus Strains		
Escherichia coli	From B. Lemaitre lab	N/A
Micrococcus luteus	From B. Lemaitre lab	N/A
Erwinia carotovora carotovora 15	From B. Lemaitre lab, (Lemaitre et al., 1997)	N/A
Enterobacter cloacae	β12, Jean Lambert, from B. Lemaitre lab, (Lemaitre et al., 1997))	N/A
Serratia marcescens	From D. Ferrandon, (Nehme et al., 2007)	N/A
Biological Samples		
N/A		
Chemicals, Peptides, and Recombinant Proteins		
OCT	Tissue-Tek	4583
Paraformaldehyde	Electron Microscopy Sciences	15710
Triton-X100	Sigma	50-904-5759
Schneider's medium	Gibco, Millipore	21720024
Complete protease inhibitor tablets	Roche	04719948001
AEBSF	Sigma	SBR00015
Fluorescently labeled phalloidin	Molecular Probes	A34055
DAPI	Sigma	D9542
DRAQ5	ThermoFisher	62252
OilRedO	Sigma	O1391
Triethylphosphate	Sigma	414050
LipidTOX dye	LifeTech	H34350
EdU	Invitrogen	E10415
FluoSpheres carboxylate modified 0.2mm	Life Technologies	F8781
E. coli K-12 Strain Bioparticles TexasRed Conjugate	Invitrogen	E2863
pHrodo *E. coli* Bioparticles	Invitrogen	P35361
TRIzol	Invitrogen	10296–010
Critical Commercial Assays		

REAGENT or RESOURCE	SOURCE	IDENTIFIER
Click-IT EdU Cell proliferation assay	Invitrogen	C10214
iScript cDNA synthesis kit	BioRad	1708891
Direct-zol RNA MiniPrep kit	Zymo Research	R2072
BioRad iTaq SYBR Green Supermix	BioRad	1725120
TaKaRa DNA Ligation Kit	Takara Bio Inc	6024
Deposited Data		
N/A		
Experimental Models: Cell Lines		
N/A		
Experimental Models: Organisms/Strains		
See Table S1		
Oligonucleotides		
See Table S2		
Recombinant DNA		
pFucci-S/G2/M Green cloning vector	MBL laboratories	AM-V9014
pFucci-G1 Orange cloning vector	MBL laboratories	AM-V9001
p-Red H-Stinger-HmlΔ-DsRed	Clark et al 2011	N/A
HmlΔFucci-G1-Orange	This paper	N/A
HmlΔFucciGreenS/G2/M-Green	This paper	N/A
Software and Algorithms		
Fiji image processing software	(Schindelin et al., 2012)	https://imagej.net/Fiji
Imaris Microscopy image analysis software	Oxford Instruments	N/A
Leica Application Suite (LAS) Microscopy Software	Leica Microsystems	N/A
Excel	Microsoft Office	N/A
Prism 8	Graphpad	N/A
Other		
N/A		